Award Number: W81XWH-10-1-0854

TITLE: Neural Development in tsc2-Deficient Zebrafish

PRINCIPAL INVESTIGATOR: Kevin Ess, Ph.D.

CONTRACTING ORGANIZATION: Vanderbilt University
Nashville TN 37240-0001

REPORT DATE: October 2011

TYPE OF REPORT: Annual

PREPARED FOR: U.S. Army Medical Research and Materiel Command
Fort Detrick, Maryland 21702-5012

REPORT DOCUMENTATION PAGE

Form Approved
OMB No. 0704-0188

1. REPORT DATE	2. REPORT TYPE	3. DATES COVERED
October 2011	Annual	15 September 2010 – 14 September 2011

4. TITLE AND SUBTITLE

Neural Development in tsc2-Deficient Zebrafish

5a. CONTRACT NUMBER

5b. GRANT NUMBER
W81XWH-10-1-0854

5c. PROGRAM ELEMENT NUMBER

6. AUTHOR(S)

Kevin Ess

E-Mail: kevin.ess@vanderbilt.edu

5d. PROJECT NUMBER

5e. TASK NUMBER

5f. WORK UNIT NUMBER

7. PERFORMING ORGANIZATION NAME(S) AND ADDRESS(ES)

Vanderbilt University
Nashville TN 37240-0001

8. PERFORMING ORGANIZATION REPORT NUMBER

9. SPONSORING / MONITORING AGENCY NAME(S) AND ADDRESS(ES)
U.S. Army Medical Research and Materiel Command
Fort Detrick, Maryland 21702-5012

10. SPONSOR/MONITOR'S ACRONYM(S)

11. SPONSOR/MONITOR'S REPORT NUMBER(S)

12. DISTRIBUTION / AVAILABILITY STATEMENT
Approved for Public Release; Distribution Unlimited

13. SUPPLEMENTARY NOTES

14. ABSTRACT
Abstract on next page.

15. SUBJECT TERMS
Subject terms on next page.

16. SECURITY CLASSIFICATION OF:			17. LIMITATION OF ABSTRACT	18. NUMBER OF PAGES	19a. NAME OF RESPONSIBLE PERSON
a. REPORT	b. ABSTRACT	c. THIS PAGE			USAMRMC
U	U	U	UU	28	19b. TELEPHONE NUMBER *(include area code)*

14. ABSTRACT

This DOD-funded project “Neural Development in tsc2-deficient zebrafish” has made excellent progress over the first year of funding. We have essentially completed Task 1 of our Statement of Work with a focus on Neural Development. We have also begun Task 2 determining cell autonomous phenotypes.

Using this zebrafish model of tuberous sclerosis complex, we have shown that the tsc2 gene sequence is highly conserved and also has a conserved function. The mutant tsc2vu242 allele encodes a truncated tuberin protein lacking the GAP domain. This resulted in loss of the ability to inhibit Rheb and of the TOR kinase within TOR complex 1 (TORC1). Homozygous mutant zebrafish have enlarged cells in the brain and liver. Of relevance to Task 1, forebrain neurons are poorly organized in homozygous mutants with extensive gray and white matter disorganization and ectopically positioned cells. Ongoing experiments with chimera zebrafish demonstrate that tsc2 limits TORC1 signaling in a cell-autonomous manner. However, wild-type host cells in the forebrain mislocalize in a non-cell-autonomous manner.

Overall, our results demonstrate a highly conserved role of tsc2 in zebrafish during neural development. These findings are the basis for a recently accepted manuscript “Kim et al.” published in Disease Models and Mechanisms (Appendix).

15. SUBJECT TERMS

TOR kinase signaling, TORC1, neural development, cell size

Project Number W91ZSQ9298N645

Table of Contents

Introduction

This DOD funded research project seeks to define the roles of the *tsc2* gene during development utilizing a zebrafish model of tuberous sclerosis complex (TSC) we have generated. Our research leverages the inherent experimental advantages of zebrafish to study TSC. Our planned work includes assessing the functional impact of loss of the *tsc2* gene during brain development, cell- and non-cell autonomous functions of tuberin and interactions with other genes to dissect signaling pathways impacted by altered tuberin function and increased TOR activity.

Body

Tuberous Sclerosis Complex (TSC) is a genetic disorder caused by loss of function of either the *TSC1* (encodes hamartin) or *TSC2* (encodes tuberin) genes (*1, 2*). Patients have multiorgan hamartomas. These non-malignant but abnormally differentiated cells are generally thought to underlie the morbidity and mortality seen in many patients with TSC. While impressive advances identifying downstream targets such as inhibition of the mTOR signaling pathway, current therapies remain ineffective with many patients suffering from intractable epilepsy as well as autism, developmental delay and behavioral problems.

To circumvent these limitations and catalyze new discovery, novel model systems are needed. The need led to our creation of a zebrafish model of TSC by inactivating the *tsc2* gene (*tsc2*^{vu242} allele). Our original **Tasks** were to: 1) further characterize brain pathology of a TSC zebrafish model featuring a *tsc2* null mutant, 2) study the formation of focal hamartomas in mosaic embryos generated through transplantation of *tsc2*-deficient cells and 3) investigate genetic interactions affecting the mTOR signaling pathway. As submitted, the **Statement of Work** had three tasks, each of which was proposed to take approximately one year:

Task 1. Further characterization of neural development in *tsc2* null zebrafish.

During this first year of funding we have essentially completed this Task though technical problems were identified with some of the subtasks. Our results were accepted for publication in *Disease Models and Mechanisms* (Kim et al. 2011)(*3*). As detailed in this manuscript, we found clear alterations of brain development and TOR signaling in homozygous *tsc2*$^{vu242/vu242}$ zebrafish. The use of rapamycin was able to reverse cell size defects in hepatocytes and neurons. Additional findings include rescue of TOR signaling in the brain from expression of zebrafish *tsc2* or human *TSC2* mRNA. Additional findings using heterozygous *tsc2*$^{vu242/+}$ zebrafish were very intriguing. We showed that endoplasmic reticulum “stress” mediated by tunicamycin treatment increased TOR signaling at a high level in the liver and a moderate level in the brain compared to wild-type controls. Final experiments in this publication reported initial results with cell transplantation. We showed that there appeared to be a non-cell autonomous mechanism at play as mutant *tsc2*$^{vu242/vu242}$ cells were able to cause wild-type neurons in the host brain to become mispositioned. For all experiments, rigorous statistical methods were applied and experiments repeated several times. For full experimental details, please refer to Kim et al. including all Supplemental Figures in the Appendix.

Progress on **Task 1a** includes crossing the *tsc2* mutant fish into several fluorescent expressing lines of zebrafish to identify cell type specific mechanisms. As in the Statement of Work **Task 1a**, we crossed the *tsc2* mutant line to **1)** neurogenin-GFP (expresses GFP in cortical progenitor cells), **2)** olig2-GFP (expressed GFP in precursors of oligodendrocytes) and **3)** Sox10-RFP (expresses RFP in mature oligodendrocytes and myelin).

During or initial characterization, we found that the neurogenin-GFP zebrafish clearly expresses GFP in neural progenitor cells that were identified by expression of Sox2 (Figure 1, red). While co-localization was seen in some cells using immunofluorescence, additional GFP positive cells in the brain were apparently not neural progenitors as they do not express Sox2. Given this mixed result, we did not back-cross the neurogenin-GFP line into a *tsc2* mutant line as the results would be very difficult to interpret given the wider expression pattern of GFP beyond neural progenitor cells. This transgene may have more specific expression at later stages of development but as our *tsc2* mutant fish all die by 7-9 days, this approach cannot be further used.

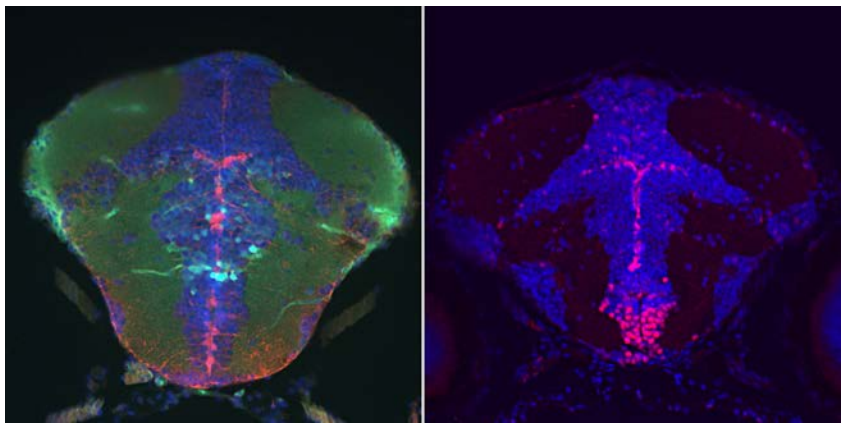

Figure 1. Expression of GFP and Sox2 in 7 day old Neurogenin-GFP zebrafish. Left: merge of Neurogenin GFP, immunofluorescence for Sox2 (red, progenitor cell marker) and DAPI (blue, nuclei) co-expression. These results show expected overlap of a subset of GFP with Sox2 cells in the brain but also reveal non-Sox2 expressing GFP cells.

Fortunately, the olig2-GFP line of zebrafish had the expected pattern of expression with clear GFP-positive processes seen in oligodendrocyte precursors in the developing central nervous system (Figure 2). We then crossed the olig2-GFP allele into wild type and *tsc2* homozygous mutant zebrafish as planned. Of note, there was a statistically significant increase in the number of oligodendrocyte precursors seen in *tsc2* mutant versus control zebrafish (Figure 3).

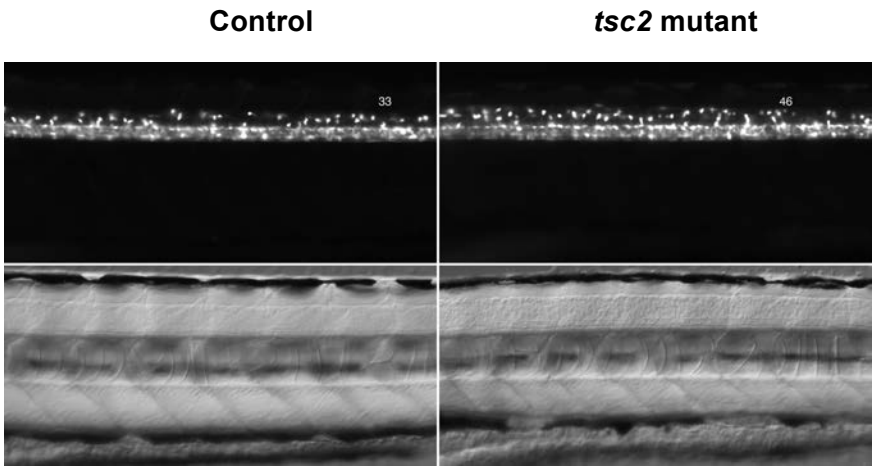

Figure 2. Expression of olig2-GFP in control (upper left) and *tsc2* mutant upper right) zebrafish reveals increased numbers of GFP-positive cells. The spinal cord also appears to be larger with shorter somites indicating an abnormality of cell size and tissue organization (control lower left, *tsc2* mutant lower right).

These results were quantitated and graphed in Figure 3.

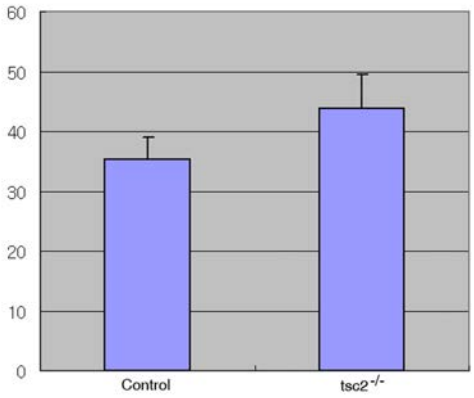

Figure 3. Increased numbers of oligo2-GFP positive processes in *tsc2* homozygous mutant zebrafish (mean 48.75, SD 6.8) versus control zebrafish (mean 32.83, SD 1.6). Using a t-test these differences were statistically significant with a *p*-value of 0.017.

Finally, we attempted to use Sox10-RFP zebrafish to investigate mature oligodendrocytes and myelin in control and *tsc2* homozygous mutant zebrafish. Unfortunately this RFP allele gave only a weak signal and thus not suitable for our experiments. Alternative fluorescent marker zebrafish for this lineage are not available.

Task 1b. We are developing a new antibody that recognizes the N-terminal of zebrafish tuberin. Development of this reagent is necessary as all commercial antibodies we have tested either use a C terminal epitope (deleted in our mutant tuberin) or do not work in zebrafish. The successful use of this new antibody will allow us to make progress on dominant-negative mechanisms as proposed in Task 1. As additional data shows a loss of *tsc2* mRNA (*3*), the allele may in fact be null. However, dominant-negative form of tuberin is possible and we have data from mRNA overexpression experiments that this is the case. An additional possibility is that while the endogenous mRNA is lost, the residual protein could be stabilized and gain potentially able to participate as a pathologic dominant negative. The antibody we are developing above will allow us to see if the truncated protein is stabilized and if so, able to have a dominant negative function. We expect to report on this intriguing mechanism in the next progress report if our efforts to make a specific antibody are successful.

Ongoing Tasks:

Task 2. Mosaic analysis of *tsc2* function by transplantation of green fluorescent protein labeled *tsc2*$^{vu242/vu242}$ cells into wild-type embryos.

As stated above, we have done initial experiments with transplantation and creation of mosaic zebrafish. These experiments are underway and by design take a prolonged period of time as we proposed to look at 6 month and 1 year timepoints.

Task 3. Genetic interactions of *tsc2* with other regulators of mTOR signaling.

This task is expected to be completed during year 3 of this grant. However, we have already started the required breeding of each line (maintenance of *ptena*, *ptenb*, *tp53* mutants and breeding to heterozygous *tsc2*$^{vu242/+}$ zebrafish).

Key Research Accomplishments

-Completion of Task 1 and acceptance of results for publication.

-Develop methodology and assays for transplantation experiments, creation of mosaic zebrafish that is key for Task 2 (planned Year 2).
-Obtain multiple genetically altered zebrafish (*ptena*, *ptenb*, *tp53* mutants) and begin breeding into *tsc2* mutant backgrounds for Task 3 (planned Year 3).

Reportable Outcomes

1. Publication of our work in *Disease Models and Mechanisms* (*3*)
2. Oral presentation of results (by PI Kevin Ess) at an International Meeting (7th European Zebrafish Meeting, Scotland July 2011).

Conclusion

This first year of funding has been very successful with overall achievement of scientific goals as well as outcomes as detailed for Task 1. The next year will continue as planned with further experiments on mosaic zebrafish and genetic interactions of the zebrafish *tsc2* gene with additional genes. These will allow us to define mechanisms relevant to TSC as well as normal brain development. Our continued progress will be the foundation of additional grant submissions to NIH. We anticipate a 2012-2013 submission of our next proposal for 5 years of R01 level funding. Obtaining future grants will allow us to continue this project initiated by DOD funding past 2013.

To address why our research is important, we are in a unique position to rapidly generate new knowledge that is extremely relevant to patients with TSC. This significance extends well beyond the field of TSC research given the central role of mTOR/TOR signaling as this pathway has many important roles during the development of multiple organs as well as during disease pathogenesis. The use of zebrafish as our model organism here will greatly facilitate experiments that will examine genetic interactions, non-cell autonomous function of mutant cells and possibly dominant-negative mechanisms. All of these approaches are extremely relevant to TSC and will clearly change our approach to this disease and other abnormalities that include aberrant mTOR/TOR signaling.

References

1. P. B. Crino, Rapamycin and tuberous sclerosis complex: from Easter Island to epilepsy. *Ann Neurol* **63**, 415 (Apr, 2008).
2. K. Ess, Tuberous Sclerosis Complex: A Brave New World? *Current Opinion in Neurology* **23**, 189 (2010).
3. S. H. Kim, C. K. Speirs, L. Solnica-Krezel, K. C. Ess, Zebrafish model of tuberous sclerosis complex reveals cell-autonomous and non-cell-autonomous functions of mutant tuberin. *Dis Model Mech* **4**, 255 (Mar, 2011).

Appendix (next page)

(Kim, Speirs, Solnica-Krezel and Ess. “Zebrafish model of tuberous sclerosis complex reveals cell-autonomous and non-cell-autonomous functions of mutant tuberin”, *Disease Models Mechanisms* 2011)

Supporting Data

Not applicable.

Disease Models & Mechanisms 4, 000-000 (2011) doi:10.1242/dmm.005587

Zebrafish model of tuberous sclerosis complex reveals cell-autonomous and non-cell-autonomous functions of mutant tuberin

Seok-Hyung Kim[1], Christina K. Speirs[1], Lilianna Solnica-Krezel[1] and Kevin C. Ess[2,*]

SUMMARY

Tuberous sclerosis complex (TSC) is an autosomal dominant disease caused by mutations in either the *TSC1* (encodes hamartin) or *TSC2* (encodes tuberin) genes. Patients with TSC have hamartomas in various organs throughout the whole body, most notably in the brain, skin, eye, heart, kidney and lung. To study the development of hamartomas, we generated a zebrafish model of TSC featuring a nonsense mutation (*vu242*) in the *tsc2* gene. This $tsc2^{vu242}$ allele encodes a truncated Tuberin protein lacking the GAP domain, which is required for inhibition of Rheb and of the TOR kinase within TORC1. We show that $tsc2^{vu242}$ is a recessive larval-lethal mutation that causes increased cell size in the brain and liver. Greatly elevated TORC1 signaling is observed in $tsc2^{vu242/vu242}$ homozygous zebrafish, and is moderately increased in $tsc2^{vu242/+}$ heterozygotes. Forebrain neurons are poorly organized in $tsc2^{vu242/vu242}$ homozygous mutants, which have extensive gray and white matter disorganization and ectopically positioned cells. Genetic mosaic analyses demonstrate that *tsc2* limits TORC1 signaling in a cell-autonomous manner. However, in chimeric animals, $tsc2^{vu242/vu242}$ mutant cells also mislocalize wild-type host cells in the forebrain in a non-cell-autonomous manner. These results demonstrate a highly conserved role of *tsc2* in zebrafish and establish a new animal model for studies of TSC. The finding of a non-cell-autonomous function of mutant cells might help explain the formation of brain hamartomas and cortical malformations in human TSC.

INTRODUCTION

Tuberous sclerosis complex (TSC) is a genetic disease characterized by hamartomas in multiple organs, including the brain, skin, kidney, heart and lung (Crino et al., 2006). These focal lesions represent non-malignant collections of cells that have undergone abnormal differentiation. Neurological features are generally severe, with many patients suffering from intractable epilepsy, autism, behavioral problems and mental retardation (Ess, 2006). These important neurological features are generally accepted to be due to brain hamartomas (termed 'tubers') that represent severe cortical malformations. TSC results from loss of function of either the *TSC1* (encoding hamartin) or *TSC2* (encoding tuberin) genes. Although often due to a spontaneous mutation, TSC can be inherited as an autosomal dominant disorder. According to the prevailing model, patients with TSC have an initial mutation in one copy of either the *TSC1* or *TSC2* gene, and this mutation is either inherited from a parent or spontaneously acquired early in development. A subsequent 'second hit' mutation or deletion then occurs in focal areas of various organs, leading to the development of a hamartoma. This loss of heterozygosity (LOH) model has been repeatedly demonstrated in kidney and lung hamartomas from patients with TSC, but supporting data in the brain has been quite elusive (Henske et al., 1996). These findings have led to proposals of alternative pathways of disease progression, including haploinsufficiency, post-translational modification of the TSC gene products (Ma et al., 2005) and possible dominant-negative action of certain mutant alleles (Govindarajan et al., 2005).

The *TSC1* and *TSC2* genes were named after genetic linkage studies determined that there were two independent loci that could cause TSC. Their gene products are essentially unrelated, possessing sequence homology only in their coiled-coil domains that mediate protein-protein interactions. Indeed, compelling evidence gathered over the last several years shows that hamartin and tuberin bind to one another forming a complex that can then inhibit the G protein Rheb, an activator of the TOR (target of rapamycin) serine/threonine kinase (Inoki et al., 2003; Zhang et al., 2003). In mammals, mTOR (mammalian TOR) is found within multiprotein complexes termed mTORC1 (contains Raptor and is highly sensitive to rapamycin) or mTORC2 (contains Rictor and is relatively rapamycin insensitive) (reviewed in Huang and Manning, 2008). The hamartin-tuberin–Rheb–TOR pathway is highly conserved in *Drosophila*, yeast, mice and humans (Nobukini and Thomas, 2004; van Slegtenhorst et al., 2004), with the mTORC1 signaling pathway being constitutively upregulated in TSC patients (Crino et al., 2006). The identification of mTOR as a key signaling pathway regulated by hamartin-tuberin greatly aided research in the pathogenesis of TSC and its role during development. Active areas of current research are delineating the functions of mTOR within mTORC1 and mTORC2 (Huang and Manning, 2009) and how dysregulation of these complexes leads to human neurological disease. This burgeoning information coupled with established mouse and rat models of TSC has fuelled translational research,

[1]Vanderbilt University, Department of Biological Sciences, Nashville, TN 37232, USA
[2]Vanderbilt University Medical Center, Department of Neurology, Nashville, TN 37232, USA
*Author for correspondence (kevin.ess@vanderbilt.edu)

Received 21 March 2010; Accepted 16 September 2010

leading to the use of mTORC1 inhibitors as therapeutics for TSC (Bissler et al., 2008; Davies et al., 2008; Franz et al., 2006; Zhou et al., 2009).

Although mutations in either *TSC1* or *TSC2* are sufficient to cause dysregulation of mTOR, patients with *TSC2* mutations often manifest more severe disease than those with *TSC1* mutations, suggesting that there are additional functions of tuberin that are currently unknown (Au et al., 2007). Multiple rodent models of TSC have been developed to study *Tsc1* and *Tsc2* gene function. Although informative, conventional homozygous mouse knockouts of either *Tsc1* or *Tsc2* are lethal by embryonic day 12 (Kobayashi et al., 1999; Kobayashi et al., 2001; Onda et al., 1999). Such studies shed only limited light on the pathogenesis of brain hamartomas in TSC because these homozygous mutant mice die prior to any substantive stages of cortical development. Mice that are heterozygous for *Tsc1* or *Tsc2* mutations develop kidney pathology by 6-12 months of age but exhibit only minimal brain pathology (Onda et al., 1999; Uhlmann et al., 2002a). Similar results were seen for the Eker rat, a long-studied model of kidney disease that is due to an insertional mutation within the rat *Tsc2* gene (Kobayashi et al., 1995). Comparable to the situation in mice, homozygous *Tsc2*-deficient Eker rats manifest an early embryonic-lethal phenotype, whereas heterozygous animals have minimal CNS manifestations (Tschuluun et al., 2007). To circumvent these limitations and study abnormalities in postnatal mice, multiple conditional-knockout models of TSC have been established by inactivating the *Tsc1* or *Tsc2* genes in specific cell types, including in neurons and astrocytes (Uhlmann et al., 2002b; Way et al., 2009; Wong et al., 2003). Although these approaches have better defined the role of specific CNS lineages in TSC, they have not adequately modeled tuber formation in the brain.

Zebrafish are a compelling model in which to study the role of the *TSC1* and *TSC2* genes as well as the pathogenesis of TSC. This is owing to the many experimental advantages offered by zebrafish, including the ability to observe directly embryonic development, ease of cell transplantation and the many genetic tools available to identify specific populations of CNS cell types (Baraban et al., 2007; Cooper et al., 2005). Use of zebrafish to study TSC has been limited to date to two characterized *TSC1* homologs (DiBella et al., 2009). In this study, the authors used antisense morpholino oligonucleotides to knock down function of the zebrafish *tsc1a* gene, and found a role in the control of cilia length and kidney development. However, these experiments did not address whether loss of zebrafish *tsc1* causes abnormalities of cell size or its impact on brain development.

To define the role of tuberin during development, we cloned and characterized the expression of the zebrafish *tsc2* gene. We then used TILLING (targeting induced local lesions in genomes; supplementary material Fig. S1) (Till et al., 2003) to identify zebrafish that harbor a *tsc2* nonsense mutation. This $tsc2^{vu242}$ mutant allele encodes a truncated form of Tuberin, lacking the highly conserved GTPase-activating protein (GAP) domain that mediates Rheb inactivation and TORC1 inhibition. Homozygous $tsc2^{vu242/vu242}$ mutants died during early larval stages, manifesting multi-organ pathology with increased cell size and ectopically positioned cells within the forebrain. Greatly increased levels of TORC1 were seen in mutant embryos, and treatment of mutant larvae with rapamycin, a potent TORC1 inhibitor, reversed the defects in cell size, indicating that the role of Tuberin in the TOR pathway is highly conserved in zebrafish. Although heterozygous $tsc2^{vu242/+}$ fish are viable and morphologically normal, they showed moderate increases in TORC1 signaling. This finding and additional evidence suggests that a threshold of increased TOR signaling is required to cause pathology. Finally, transplantation of mutant cells to wild-type hosts revealed both cell-autonomous and non-cell-autonomous forebrain abnormalities. Overall, our studies reveal that the Tsc2-TOR pathway is highly conserved in zebrafish and demonstrate the utility of zebrafish for defining pathological mechanisms that lead to complex multi-organ disorders such as TSC.

RESULTS

Expression pattern of *tsc2* during zebrafish development

To better understand the role of *TSC2* in normal development and disease, we first cloned full-length zebrafish *tsc2* cDNA. The predicted protein overall shows 60% identity and 73% similarity to human tuberin (supplementary material Fig. S2). The hamartin-interacting, tuberin and GAP domains are all highly conserved, with 71%, 70% and 75% identical amino acids between the two species, respectively (Fig. 1M). Analysis of the spatiotemporal expression pattern by whole-mount in situ hybridization revealed that *tsc2* transcripts are maternally deposited (Fig. 1A) and ubiquitously expressed during blastula, gastrula and segmentation stages (Fig. 1B-D). By 25 hours post-fertilization (hpf), *tsc2* expression is highly enriched in the developing eye, forebrain, midbrain, lateral hindbrain region and otic vesicles (Fig. 1E-G), as well as in the blood vessels (Fig. 1H). At 36 hpf, strong expression persists in the brain (Fig. 1I) and transverse sections show that *tsc2* is also expressed in the ventrolateral region of the hindbrain (Fig. 1J). At 3 days post-fertilization (dpf), we detected low levels of *tsc2* expression in the eye (Fig. 1K), heart and intestine, in addition to the continued higher levels in the brain (Fig. 1L).

Generation of fish harboring a nonsense mutation in the *tsc2* gene

To study loss of *tsc2* function in zebrafish, we employed TILLING to identify *N*-ethyl-*N*-nitrosourea (ENU)-induced mutations in the *tsc2* gene (supplementary material Fig. S1). By screening 4608 ENU-mutagenized F1 zebrafish (Mullins et al., 1994; Solnica-Krezel et al., 1994), we found one fish heterozygous for C to A transversion, predicted to change the normal tyrosine (Y) residue at amino acid 1031 to a premature stop codon (Fig. 1M). Because this $tsc2^{vu242}$ nonsense mutation is predicted to remove the GAP domain but retain the Hamartin-binding domain, we hypothesized that the truncated protein will have either null or possibly dominant-negative activity (Govindarajan et al., 2005). Because the C-terminus of Tuberin contains the epitope for all currently available anti-Tuberin antibodies, one consequence of the $tsc2^{vu242}$ nonsense mutation is an inability to perform immunofluorescence and western blotting experiments to determine expression levels and localization of Tuberin protein. However, we confirmed the existence of mutant Tuberin by using an antibody directed against phospho-Tuberin (Ser939), because the mutant Tuberin retains this N-terminal epitope. Notably, the expression levels of phospho-Tuberin (Ser939) were not appreciably changed between wild-type and heterozygous or homozygous mutant fish at 32 hpf (supplementary material Fig.

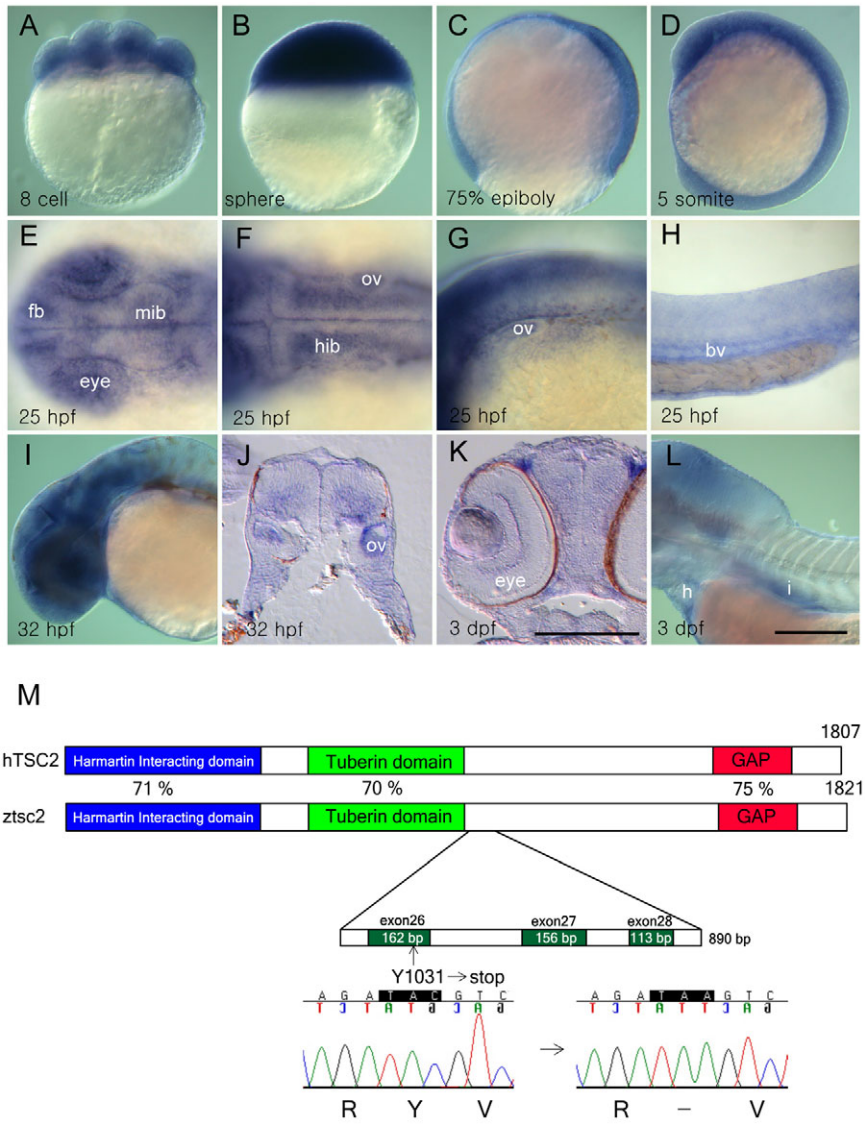

Fig. 1. Zebrafish *tsc2* is maternally and zygotically expressed during development. (A-D) Ubiquitous expression of wild-type *tsc2* at the eight-cell (A), sphere (B), 75% epiboly (C) and five-somite (D) stage. (E-H) At 25 hpf, *tsc2* expression is detected in discrete regions of the developing eye and forebrain and midbrain (E), lateral part of the hindbrain (F), otic vesicle (F,G), pharyngeal arch (G), and blood vessels (H). (I) At 32 hpf, *tsc2* expression is maintained in the eyes and brain. (J) Transverse section of the hindbrain region shows that *tsc2* expression is limited to the ventrolateral region in wild-type embryos. (K,L) At 3 dpf, *tsc2* expression is detected in the eye (K), heart and intestine (L). (M) Structure of the predicted protein domains of wild-type human *TSC2* and zebrafish *tsc2*. The *vu242* mutation causes a premature stop codon within exon 26. Blue indicates the hamartin-interacting domain, green the tuberin domain and red the GAP domain. fb, forebrain; mib, midbrain; hib, hindbrain; bv, blood vessel; h, heart; i, intestine; ov, otic vesicle. Scale bars: 250 μm (bar in K is for J, K; bar in L is for A-I, L). (A-D,H,I,L) Lateral views; (E,F) dorsal views; anterior to the left.

S3). To more precisely define Tuberin stability in wild-type and heterozygous or homozygous mutant fish, new antibodies that specifically recognize the N-terminus of zebrafish Tuberin will need to be generated.

Early lethality, enlarged liver and increased TORC1 activity in *tsc2*$^{vu242/vu242}$ mutants

tsc2$^{vu242/vu242}$ homozygous mutant embryos and subsequent larvae did not develop overt morphological defects until 5 dpf, although a few homozygous mutants did not fully inflate their swim bladder. The most prominent phenotype was then manifest by 7 dpf, when *tsc2*$^{vu242/vu242}$ mutant zebrafish exhibited completely deflated swim bladders and enlarged livers (Fig. 2C,D,L). All mutant embryos died by 11 dpf, possibly because of limited food intake that might be due in part to the swim bladder abnormalities or abnormal brain morphology and/or function (see below). *tsc2*$^{vu242/+}$ heterozygous fish are viable, develop into fertile adults and have no discernable phenotype. Therefore, *tsc2*^{vu242} seems to act as a recessive embryonic-lethal mutation in zebrafish.

To determine whether *tsc2*^{vu242} mutation causes abnormalities of TOR kinase signaling, we evaluated the phosphorylation status of S6 ribosomal protein and 4E-BP1 because these proteins are well-established downstream effectors of the mTOR kinase within the mTORC1 complex (Inoki et al., 2002). Immunohistochemistry on 7-dpf embryos using antibodies specific to phospho-S6 and phospho-4E-BP1 showed that the *tsc2*$^{vu242/vu242}$ mutant embryos exhibited highly increased levels of both phosphoproteins in several organs, including in cells in the eye, brain and spinal cord (Fig. 2E-J), liver (Fig. 2L), intestine (Fig. 2L,P), and kidney (Fig. 2P), as compared with wild-type siblings (Fig. 2A,B,E-G,K,M,N). The elevated TORC1 activity was suppressed by injection of wild-type zebrafish *tsc2* and at least partially suppressed with wild-type human *TSC2* RNA (supplementary material Fig. S4). We next performed western blotting to evaluate levels of activation of the TORC1 pathway in protein extracts from *tsc2*$^{vu242/vu242}$ homozygous, *tsc2*$^{vu242/+}$ heterozygous and wild-type embryos at 7 dpf (Fig. 2Q). Consistent with immunohistochemistry results, phospho-4E-BP1 and phospho-S6 levels were highly elevated in

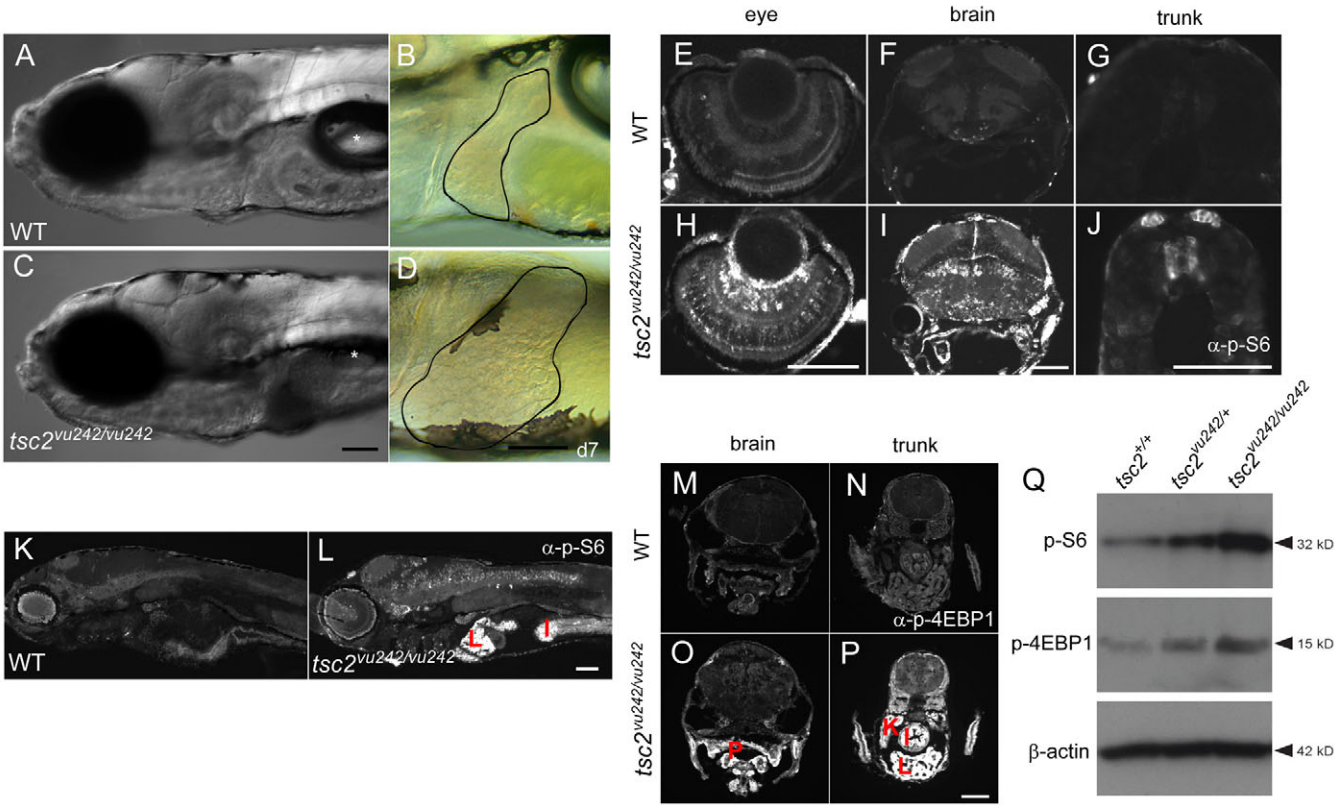

Fig. 2. Upregulation of TORC1 activity in various tissues of *tsc2*$^{vu242/vu242}$ mutants. (A-D) Homozygous mutant zebrafish have a deflated swim bladder and markedly enlarged liver at 7 dpf. Livers are outlined (B,D); asterisk indicates swim bladder. (E-P) Sections obtained from wild-type (WT) and *tsc2*$^{vu242/vu242}$ embryos at 7 dpf and stained with anti-phospho-S6 ribosomal protein (Ser235/236) antibody (E-L) or anti-phospho-4E-BP1 (Thr37/46) (M-P). Phospho-S6 staining in the eye (E,H), brain (F,I) and trunk (G,J). Phospho-4E-BP1 staining in the brain (M,O) and trunk (N,P). (Q) Western blot using anti-phospho-S6 ribosomal protein antibody and anti-phospho-4E-BP1 of total protein lysates from 7-dpf wild-type, *tsc2*$^{vu242/+}$ and *tsc2*$^{vu242/vu242}$ larvae. Antibody staining for β-actin was used as a loading control. P, pharynx; K, kidney; I, intestine; L, liver. Scale bars: 100 μm.

tsc2$^{vu242/vu242}$ homozygotes. These results indicate that activation of the TORC1 pathway as a consequence of decreased *tsc2* function is conserved in zebrafish. We also detected a moderate increase of TORC1 signaling (phospho-S6 and phospho-4E-BP1) in heterozygous larvae when compared with wild-type siblings (Fig. 2Q). Notably, *tsc2*$^{vu242/+}$ heterozygotes showed no overt morphological defects, including cell size, despite this enhancement of TORC1 activation, implying a threshold above which TOR signaling can affect organ development. This increased TORC1 activity in *tsc2*$^{vu242/+}$ heterozygotes is consistent with a mechanism of haploinsufficiency of the remaining wild-type allele. This has been previously demonstrated in mouse models of TSC (Ehninger et al., 2008).

Overexpression of truncated Tuberin in wild-type embryos increases TORC1 activity and alters brain development

To test whether the *tsc2*^{vu242} nonsense mutation can interfere with TORC1 signaling, we overexpressed full-length or truncated Tuberin by injecting synthetic wild-type *tsc2* or *tsc2*^{vu242} RNA, or an additional truncated-Tuberin-encoding RNA, into wild-type embryos at the one-cell stage. We observed enlarged cells in the superficial enveloping layer in embryos injected with 400 pg of *tsc2* RNA containing the *tsc2*^{vu242} nonsense mutation, and these cells had increased levels of phospho-S6 during early development (10-11 hpf) (Fig. 3C,G) compared with wild type. A similar phenotype was also generated by overexpressing a similar truncated form of Tuberin, made from a *Nru*I deletion construct of wild-type *tsc2* (Fig. 3D,H). By contrast, embryos injected with 300 pg of wild-type *tsc2* RNA did not show such abnormalities (Fig. 3B,F). These results suggested that truncated Tuberin generated by the *tsc2*^{vu242} nonsense mutation or a deletion construct might interfere with the function of endogenous Tuberin. By 27 hpf, abnormal brain morphology with a dorsally expanded hindbrain was observed in embryos injected with RNA encoding the truncated forms of Tuberin (Fig. 3K,L) but not in those injected with wild-type *tsc2* RNA (Fig. 3J). In addition, we observed slightly decreased levels of *tsc2* transcripts in heterozygous fish and a marked decrease in homozygous mutants at 26 hpf (supplementary material Fig. S5E,F). Given the position of the premature stop codon, this is probably caused by nonsense-mediated mRNA decay (NMD) (Silva and Romao, 2009). Although levels of mutant Tuberin could then decrease over time compared with wild-type Tuberin, the amount of phospho-Tuberin (Ser939) protein (supplementary material Fig. S3) was relatively stable in mutant larvae at 26 hpf.

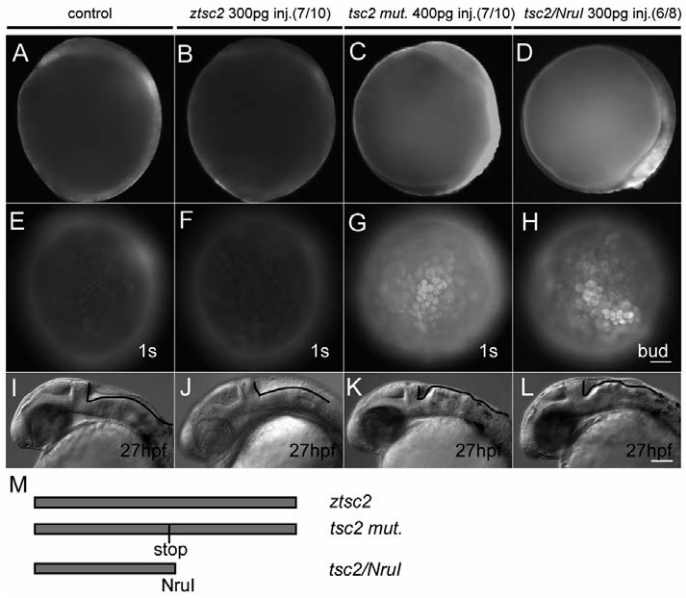

Fig. 3. Ectopic expression of truncated forms of Tsc2 increases TORC1 activity and causes morphological defects in the brain. (A-D) Lateral view of uninjected wild-type control (A), *tsc2* wild-type RNA-injected (B), *tsc2*^{vu242} RNA-injected (C) and *tsc2/Nrul*-truncated RNA-injected (D) embryos at the one-somite stage (10.3 hpf). Embryos were labeled with an antibody to phospho-S6 (A-H). (E-H) Dorsal view of A-D. (I-L) Lateral views (anterior to the left) of control (I), *tsc2* RNA-injected (J), *tsc2*^{vu242} RNA-injected (K) and *tsc2/Nrul*-truncated RNA-injected (L) embryos at 27 hpf. Solid lines mark the hindbrain boundary (I-L). (M) Schematic of constructs used for the production of synthetic RNAs for injection experiments. Scale bars: 100 μm.

tsc2$^{vu242/vu242}$ mutants have larger hepatocytes and neurons

The enlarged liver seen in *tsc2*$^{vu242/vu242}$ mutant larvae (Fig. 2C,D) could result from either increased numbers or size of hepatocytes. Using BrdU-incorporation experiments, we did not detect increased cell proliferation in *tsc2*$^{vu242/vu242}$ mutants compared to wild-type embryos by 7 dpf (data not shown). To measure cell size, we crossed *tsc2*$^{vu242/+}$ carriers with fish harboring the *Tg(β-actin:mGFP)* transgene, which expresses green fluorescent protein (GFP) at the cell membrane in all tissues under the control of the β-actin promoter (Cooper et al., 2005). We crossed the resulting *tsc2*$^{vu242/+}$*;Tg(β-actin:mGFP)* fish and determined cell size in *tsc2*$^{vu242/vu242}$ homozygous mutants in various organs at 9 dpf. These analyses revealed increased size of hepatocytes by approximately twofold in *tsc2*$^{vu242/vu242}$ homozygous mutants as compared with wild-type siblings (Fig. 4A,B,G).

We also observed that the spinal cord in *tsc2*$^{vu242/vu242}$ mutants at 7.5 dpf was clearly larger than that in wild-type siblings (Fig. 4E,F,I). To clarify again whether the spinal cord phenotype resulted from enlarged neuronal cells bodies or an increased number of neurons, we measured cell area (Fig. 4H) and counted the number of cell nuclei in the spinal cord (Fig. 4J) of *Tg(β-actin:mGFP)* transgenic wild-type and mutant embryos. These analyses revealed that neuronal cell bodies in the brain and spinal cord of *tsc2*$^{vu242/vu242}$ mutants were approximately 1.5-times larger than wild-type neurons (Fig. 4C-F,H). However, there was no change in the number of spinal cord neurons (Fig. 4J). These results indicate that *tsc2* mediates cell size rather than cell proliferation in the liver and spinal cord during embryogenesis.

Rapamycin treatment dose-dependently suppresses increased cell size in *tsc2*$^{vu242/vu242}$ mutant zebrafish

To determine what aspects of the *tsc2*$^{vu242/vu242}$ mutant phenotype are due to excess TORC1 signaling, we employed rapamycin, a specific inhibitor of mTORC1 (Huang and Manning, 2008). In zebrafish, rapamycin treatment before 3 dpf causes a general developmental delay and seems to specifically interfere with intestinal development (Makky et al., 2007). To avoid such adverse effects, we started rapamycin treatment at 3.5 dpf using rapamycin concentrations ranging from 5-1000 nM. After 24 hours of rapamycin treatment, embryos were genotyped and transverse trunk sections were examined for TORC1 signaling by determining levels of phospho-S6 using immunofluorescence. We observed a dose-dependent reduction of phospho-S6 levels in the mutant embryos (Fig. 4K). After 4 days of rapamycin treatment, the phenotype of enlarged hepatocytes seen in 7-dpf *tsc2*$^{vu242/vu242}$ mutants was also suppressed in a dose-dependent manner, with normalization of hepatocyte size seen with 50 nM of rapamycin (Fig. 4L,M). Statistical analysis confirmed significant changes in each treatment condition when compared with wild-type and untreated *tsc2*$^{vu242/vu242}$-mutant control fish (Fig. 4M). Together these observations indicate the increased size of hepatocytes and liver in *tsc2*$^{vu242/vu242}$ zebrafish mutants are largely due to the elevated level of TORC1 activity during early larval stages.

Disruption of the organization of gray and white matter in the forebrain of *tsc2*$^{vu242/vu242}$ zebrafish

Almost all patients with TSC have structural brain lesions that include cortical tubers, white matter abnormalities, subependymal nodules and subependymal giant cell astrocytomas (Bourneville, 1880; Mizuguchi, 2001). To investigate whether the forebrain architecture in zebrafish is affected by the inactivation of *tsc2*, we collected coronal sections of wild-type and *tsc2*$^{vu242/vu242}$ homozygous mutant larvae at 7.5 dpf (Fig. 5). In the wild-type forebrain, the structure of pallium and the dorsal division of subpallium were well developed with a clear boundary between the gray and white matter (Fig. 5A,B; *n*=14/15). The telencephalic ventricle was also clearly defined (Fig. 5A). By contrast, the corresponding brain regions in the *tsc2*$^{vu242/vu242}$ mutants showed poorly defined midline structures of the gray matter and telencephalic ventricles (Fig. 5E). The pallium and dorsal subpallium were also disorganized and less compact in *tsc2*$^{vu242/vu242}$ mutants compared with wild type (Fig. 5E; *n*=18/18), reminiscent of the abnormal cortical lamination seen in patients with TSC (Crino, 2004). Moreover, the white matter between pallium and dorsal subpallium was disrupted by numerous scattered neuronal cell bodies, suggestive of abnormal neuronal migration (Fig. 5E,F). In zebrafish, this region is homologous to the dorsal mammalian brain at the interface between cortex and subcortical white matter (Mueller and Wullimann, 2009). The dorsal subpallium was also wider in the mutants but the average number of cells in this region was not significantly changed (data not shown), suggesting that this tissue was poorly organized and less compact than in the corresponding wild-type dorsal subpallium. The most anterior part

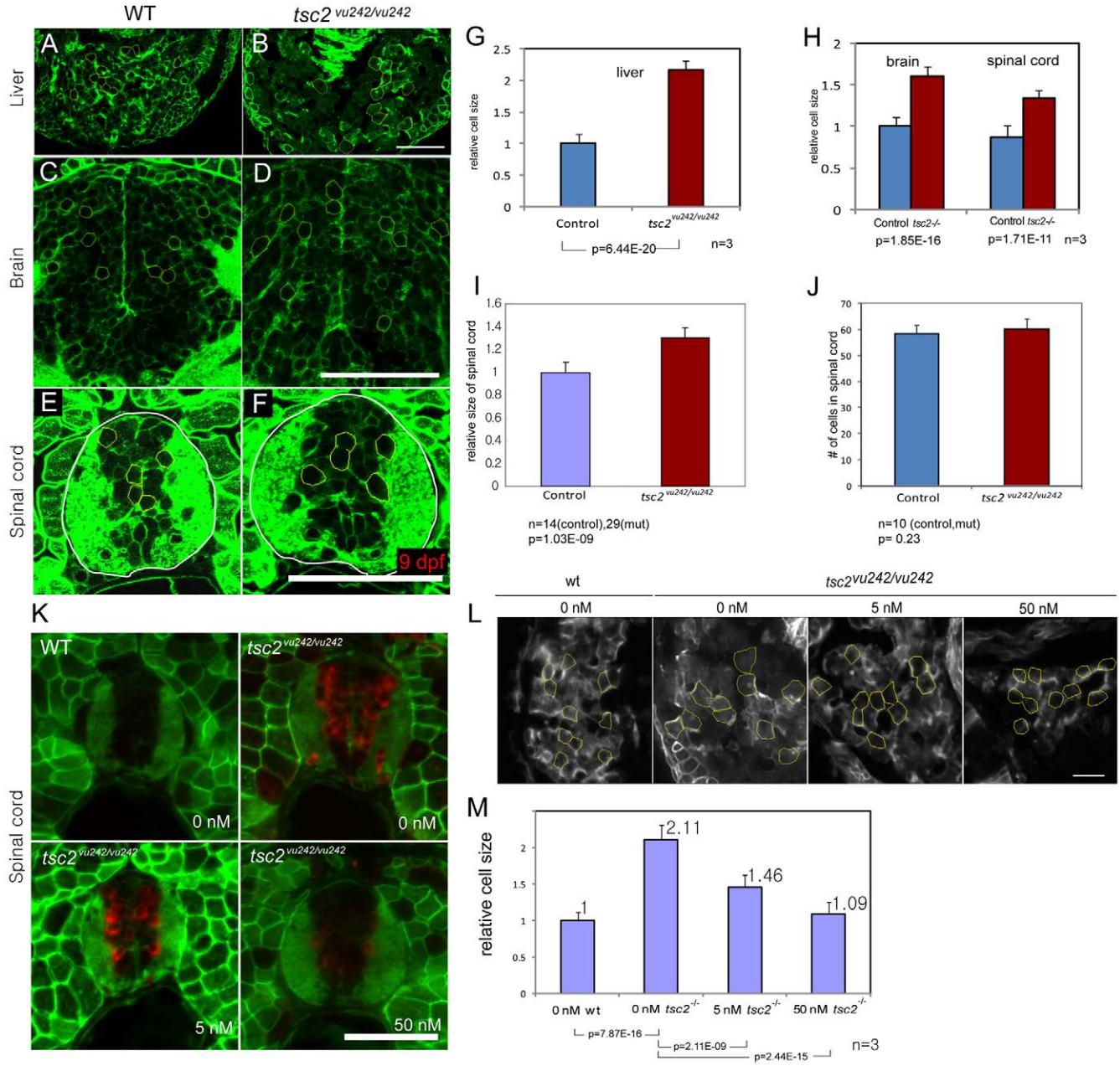

Fig. 4. Enlarged hepatocytes and brain and spinal cord neurons in *tsc2*$^{vu242/vu242}$ mutant zebrafish and suppression of hepatocyte size by inhibition of TORC1 activity. (A-F) Transverse section of liver (A,B), brain (C,D) and spinal cord (E,F). (G) Hepatocyte size differences in control siblings and *tsc2*$^{vu242/vu242}$ mutants are shown. (H) The relative size of neuronal cells in the brain and spinal cord were compared. (I) Homozygous mutant zebrafish have increased size of their spinal cord. (J) Cell number within the spinal cord in control and *tsc2*$^{vu242/vu242}$ mutants. (K) Transverse sections through the trunk of 4.5-day-old embryos treated with different concentrations of rapamycin from 3.5 dpf to 4.5 dpf were stained with antibody to phospho-S6 (red). (L) Transverse section of livers from wild-type and *tsc2*$^{vu242/vu242}$ mutants without rapamycin treatment, or with 5 nM or 50 nM rapamycin treatment. Cells outlined in yellow were measured and soma size compared. (M) Graph of measurements of relative sizes of cells from embryo shown in L. Numbers on the each bar represent relative cell size. Statistical significance of each analysis is indicated at the bottom of the graph. Scale bars: 50 μm.

of the diencephalon was also disorganized, including the pallium, eminentia thalami and the lateral forebrain bundle area (Fig. 5C,D,G,H). Finally, we analyzed more-posterior structures of the mutant brain. We did not detect any significant defects in the morphology of the posterior diencephalon extending to the hindbrain region of *tsc2*$^{vu242/vu242}$ mutants relative to wild-type siblings (supplementary material Fig. S6). These observations indicate that the anterior part of the forebrain was preferentially affected in *tsc2*$^{vu242/vu242}$ mutants compared with posterior brain regions.

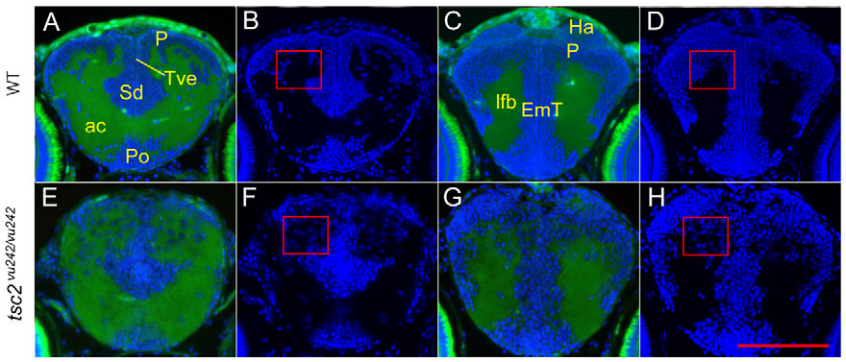

Fig. 5. Disruption of the gray and white matter in the anterior forebrain of *tsc2*$^{vu242/vu242}$ mutants. Cross-sections through the anterior forebrain of wild-type larvae (A-D) and *tsc2*$^{vu242/vu242}$ mutant larvae (E-H) at 7.5 dpf. A restricted telencephalon area containing gray and white matter was analyzed in wild-type (A,B) and *tsc2*$^{vu242/vu242}$ mutant (E,F) larvae at 7.5 dpf. (B,F) DAPI-channel-alone image of A and E. The most anterior diencephalon of the wild-type is shown in C and mutant in G, with DAPI channel in D and H. Rectangles in F and H indicate disrupted pallium layers and ectopically mis-positioned cells within the white matter. Green color is tissue autofluorescence; blue is DAPI staining. P, pallium; Po, preoptic region; Sd, dorsal division of subpallium; Tve, telencephalic ventricle; ac, anterior commissure; Ha, habenula; EmT, eminentia thalami; lfb, lateral forebrain bundle. Scale bar: 100 µm.

Cell-autonomous and non-cell-autonomous functions of mutant Tuberin in the forebrain

The disruption of gray and white matter organization that we found in the pallium, subpallium and thalamic regions could be caused by intrinsic loss of *Tsc2*, but the heterogeneity of human tubers suggests that additional mechanisms might be possible. To address this issue, we made mosaic zebrafish by transplanting *tsc2*$^{vu242/vu242}$ cells into wild-type host embryos (schematic in Fig. 6A). Donor cells were obtained from a *tsc2*$^{vu242/+}$*;Tg(h2afv:GFP)* transgenic line, in which all cell nuclei express GFP (Pauls et al., 2001). *Tsc2*$^{vu242/+}$*;Tg(h2afv:GFP)* fish were intercrossed and their progenies were used as donor embryos in the transplantation experiment (Fig. 6B-N). During transplantations at the late blastula stage (4 hpf), donor cells were taken from the animal pole region and transplanted to the same region because most of the cells in this region normally give rise to forebrain and retina (Woo and Fraser, 1995). Analyses of chimeric embryos at 7.5 dpf revealed that *tsc2*$^{vu242/vu242}$*;Tg(h2afv:GFP)* mutant cells, marked by GFP expression in the nuclei, showed a strongly increased level of TORC1 activity, as indicated by increased levels of phospho-S6 (Fig. 6F-L; *n*=20/20). We also observed a marked disruption of gray-white matter borders in a subset of the chimeric embryos (Fig. 6I, rectangle, enlarged in J-N; *n*=3/18), similar to the phenotype observed in *tsc2*$^{vu242/vu242}$ mutants (Fig. 5E-H). Strikingly, we also noted several wild-type host cell bodies (GFP negative), which, as expected, showed no increase in phospho-S6 staining, that were surrounded by mutant cells within the lateral forebrain bundle (Fig. 6J-N). By contrast, wild-type and *tsc2*$^{vu242/+}$ cells transplanted into wild-type hosts did not have increased TORC1 signaling and did not cause any brain abnormalities (Fig. 6B-E; *n*=6/6). These results suggest that *tsc2*$^{vu242/vu242}$ homozygous mutant cells activate TORC1 in a cell-autonomous manner but also in a non-cell-autonomous manner, which can cause wild-type cells to be abnormally positioned within the white matter. Because such abnormalities are seen in the brains from patients with TSC (Park et al., 1997; Shepherd et al., 1995), this observation further supports the intriguing possibility that LOH might not be absolutely required in all cells for the formation of brain hamartomas (tubers) in TSC (Talos et al., 2008).

Generation of brain lesions after transplantation of *tsc2*$^{vu242/vu242}$ mutant cells into wild-type zebrafish

Given the predominance of rodent models of human disease and the marked difficulty in performing transplantation experiments in these models, it remains unknown whether *Tsc1* or *Tsc2* mutant cells can produce the focal brain hamartomas that are almost universally seen in patients with TSC. To address whether *tsc2*$^{vu242/vu242}$ mutant cells can produce 'tuber-like' abnormalities, we transplanted membrane GFP-tagged *tsc2*$^{+/+}$*;Tg(β-actin:mGFP)* and *tsc2*$^{vu242/vu242}$*;Tg(β-actin:mGFP)* donor cells into wild-type host embryos at the blastula stage. The resulting chimeras were raised to adulthood and sacrificed 1 year after transplantation. We analyzed transverse sections of the chimeric brains with respect to TORC1 activation and tissue architecture. These analyses revealed that the transplanted wild-type *Tg(β-actin:mGFP)* cells exhibited normal levels of TORC1 pathway activity and did not cause any obvious defects in the host brain (Fig. 7A,B). By contrast, transplanted *tsc2*$^{vu242/vu242}$*;Tg(β-actin:mGFP)* cells showed elevated levels of TORC1 activity compared with the surrounding wild-type cells (Fig. 7C,F). Moreover, we noted clusters of transplanted mutant cells in the gray-white matter boundary (Fig. 7G,H) and within the gray matter in a series of sections (Fig. 7C,D). These GFP-positive cell clusters were detected through 100 µm of contiguous sections (data not shown), suggesting that they formed an extensive cluster. There seemed to be at least two types of transplanted cells in each cell cluster: relatively small and rounded cells were present (Fig. 7E) but there were also elongated and enlarged cells with dendrites, suggestive of astrocytes and/or glial cells (Fig. 7G). We were unable to confirm the lineage of these intriguing cells because there are few antibodies currently available in zebrafish that are specific to glial cell populations. These brain lesions with mixed cell types and increased TORC1 signaling suggest the formation of brain hamartomas. Further examples of these lesions in the thalamic region are notable for evidence of further disruption of brain architecture (Fig. 7I-M). These mosaic experiments indicate that *tsc2*$^{vu242/vu242}$ mutant cells can produce local lesions with increased TORC1 signaling as well as more-extensive malformations in the adult wild-type brain.

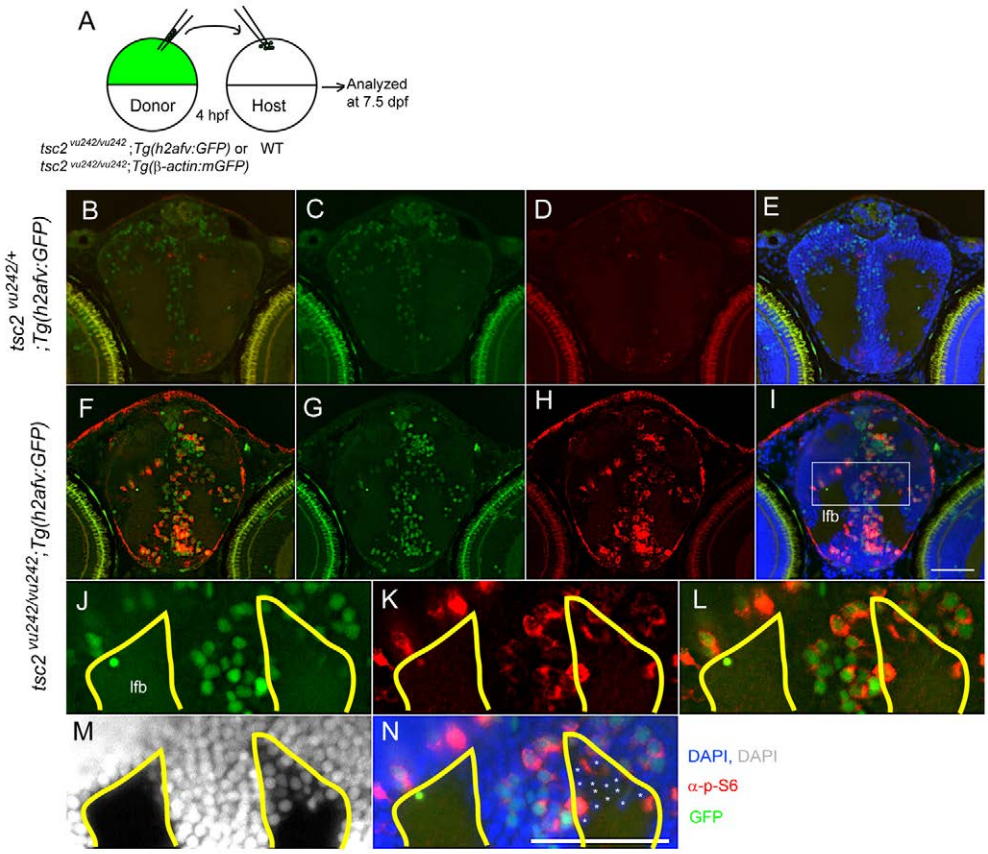

Fig. 6. Cell-autonomous activation of TORC1 in *tsc2*$^{vu242/vu242}$ mutant cells and non-cell-autonomous disruption of white matter. (A) Schematic of mosaic analyses: cells from wild-type *tsc2;Tg(h2afv:GFP)* or *tsc2*$^{vu242/vu242}$*;Tg(h2afv:GFP)* donors were transplanted into wild-type host blastulae at 4 hpf, and host embryos were analyzed at 7.5 dpf. (B-L) Coronal brain sections from wild-type embryos receiving either *Tg(h2afv:GFP)* wild-type donor cells (B-D) or *tsc2*$^{vu242/vu242}$*;Tg(h2afv:GFP)* mutant donor cells (E-L). (C,G) Green (GFP); (D,H) red (phospho-S6); (E,I) green (GFP), red (phospho-S6), blue (DAPI) merged images. (B) Merged image of C and D; (F) merged image of G and H to delineate transplanted cells and those with increased mTORC1 signaling. (J-N) Magnified views of rectangle in I. Asterisks point to wild-type host cells (GFP negative and phospho-S6 negative), which seem to be ectopically positioned within the white matter (M,N). (J-N) The area outlined in yellow marks the normal gray-white matter limits. lfb, lateral forebrain bundle. Scale bars: 50 μm.

DISCUSSION

Conserved structure and expression of zebrafish *tsc2*

TSC is a multifaceted human disease that is an important model system for the study of brain malformations as well as the pathogenesis of epilepsy and autism. Advances in these fields require relevant animal models to test hypotheses related to *TSC1* and *TSC2* gene function during development and homeostasis. Mouse models have been employed to great effect (Meikle et al., 2005; Meikle et al., 2008; Way et al., 2009; Wong, 2008), but fundamental issues concerning *TSC1* and *TSC2* function remain unanswered. In particular, the striking neurological aspects of TSC necessitate tractable model systems in which neuronal and glia differentiation can be closely examined and manipulated. To this end, we targeted the zebrafish *tsc2* gene, given the unique experimental advantages of this model organism and the marked conservation of tuberin at the amino acid level (supplementary material Fig. S2). The *tsc2*^{vu242} mutant allele described here encodes a truncated Tuberin, lacking the GAP domain, which mediates TORC1 inhibition. The resultant *tsc2*$^{vu242/vu242}$ mutants died during early larval stages, manifesting multi-organ pathology, including increased cell size in various tissues. Greatly elevated levels of TOR kinase activity were seen in *tsc2*$^{vu242/vu242}$ mutants, whereas only a moderate increase was observed in *tsc2*$^{vu242/+}$ heterozygous embryos. These heterozygous fish seem to have a normal lifespan and have a morphologically normal appearance. This suggests that there is a threshold above which increased TOR signaling causes organ pathology.

The hamartin-tuberin complex normally inhibits mammalian TORC1 activity, which controls many cellular processes, including cell growth, proliferation and differentiation (for reviews, see Huang and Manning, 2008; Huang and Manning, 2009). We found that the GAP domain of zebrafish Tuberin is also required for inhibition of zebrafish TORC1. This substantiates the concept that TOR function is highly conserved and that upstream and downstream aspects of this pathway can be effectively studied using zebrafish. One potential problem is that many genes in zebrafish have been duplicated during evolution. This can confound analyses, particularly for loss-of-function experiments. This is seen, for example, with zebrafish *tsc1,* for which two paralogs, *tsc1a* and *tsc1b* have been described (DiBella et al., 2009). However, the zebrafish *tsc2* gene does not seem to have a paralog, facilitating loss-of-function analyses as described here.

We found that the expression of *tsc2* in zebrafish is quite similar to that seen in mammals, with an early and widespread expression pattern that becomes more restricted and maximal in the central nervous system. One striking difference in zebrafish, however, is the apparent deposition of maternal *tsc2* mRNA in fertilized eggs, which is usually minimal in mammals (reviewed in Tadros and Lipshitz, 2009). This might explain why zebrafish that are homozygous for the *tsc2*^{vu242} allele can survive to approximately 11 dpf and are able to attain relatively advanced developmental stages compared with that seen for *Tsc2*-deficient mice and rats (Kobayashi et al., 1999; Kobayashi et al., 2001; Onda et al., 1999). A maternal contribution of *tsc1* or *tsc2* mRNA might further explain

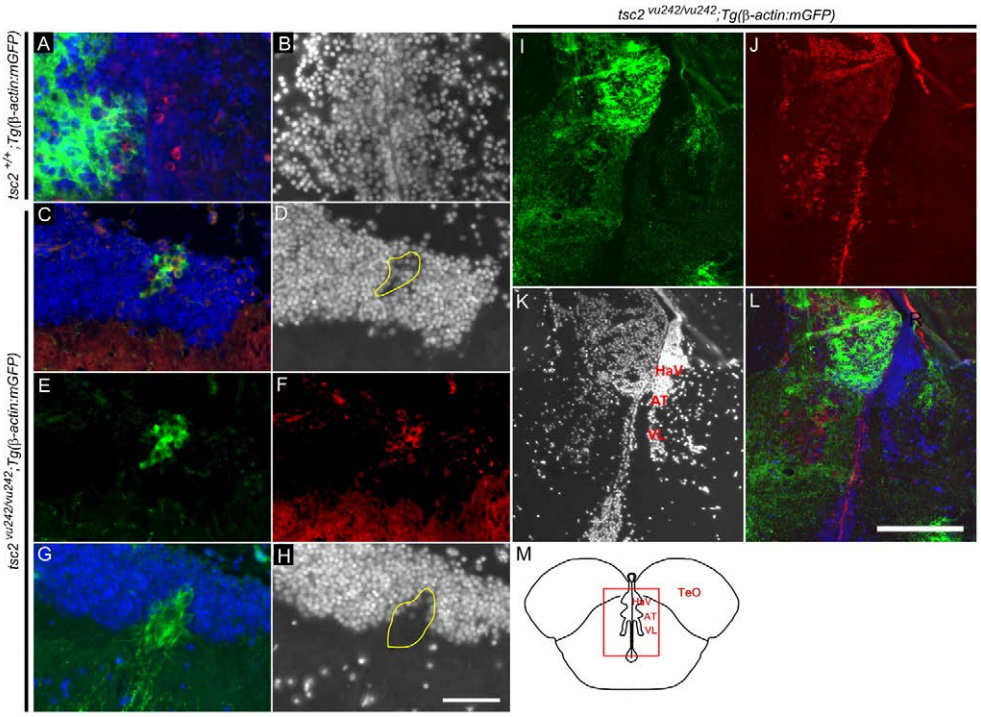

Fig. 7. Adult brain abnormalities after *tsc2*$^{vu242/vu242}$ mutant cell transplantation. (A-L) Coronal sections of adult brain at 1 year of age. (A) Green (GFP) indicates transplanted wild-type cells, blue (DAPI) shows nuclei and red shows phospho-S6 staining. (B) DAPI channel of A. (C-L) Cell clusters were found 1 year after transplantation in wild-type host zebrafish of *tsc2*$^{vu242/vu242}$*;Tg(β-actin:mGFP)* donor cells. (C,E,G,I,L) Green cells indicate transplanted *tsc2*$^{vu242/vu242}$*;Tg(β-actin:mGFP)* cells. (D,H,K) DAPI staining showing disruption of gray and white matter in wild-type host brain. (C,G) Distance between the two cortical sections shown is 50 μm. (F,J) Red shows phospho-S6 staining. (D,H) Selected areas surrounded by yellow line indicate a disruption of gray and white matter. (C) Merged image of D-F; (L) merged image of I-K. (M) Schematic of brain structure (rectangle) for I-L. TeO, tectum opticum; HaV, ventral habenular nucleus; AT, anterior thalamic nucleus; VL, ventrolateral thalam. Scale bars: 50 μm (A-H); 200 μm (I-L).

why 'knock-down' experiments directed against *tsc1* using translation-blocking antisense morpholino oligonucleotides were associated with an earlier onset of and more-severe phenotypes (DiBella et al., 2009) (and our unpublished data). Alternatively, unlike in mammals, the *tsc2* gene might not be absolutely required during early zebrafish development. Definitively addressing this issue will require the generation of zebrafish embryos lacking expression of both maternal and zygotic *tsc2* genes.

Zebrafish *tsc2* limits TOR activity and regulates cell size during development

On the basis of pathological data from patients with TSC, crucial aspects of any relevant model of TSC include elevated TOR (mTOR) activity and increased cell size within mutant organisms. This second feature should then be reversible by treatment with TORC1 (mTORC1) inhibitors such as rapamycin (Meikle et al., 2008; Zeng et al., 2008). Our zebrafish *tsc2*$^{vu242/vu242}$ embryos fulfill both these criteria, with dysregulated TORC1 signaling, as evidenced by increased levels of phospho-S6 and phospho-4E-BP1. Although this is seen in various organs throughout the mutant embryos, the greatest upregulation was detected in the brain and liver. Additional evidence for increased TORC1 signaling is provided by the enlarged size of neurons and hepatocytes in *tsc2*$^{vu242/vu242}$ zebrafish. This increased cell size was normalized by treatment with rapamycin at low concentrations, indicating TORC1 dependence (Fig. 4). These findings underscore the striking conservation of *tsc2* sequence, as well as function, throughout evolution. In addition, these findings highlight the utility of zebrafish for the study of TSC and other human disorders resulting from dysregulation of the TOR kinase. It should be noted that not all cells of the *tsc2*$^{vu242/vu242}$ mutant zebrafish are increased in size. Whereas hepatocytes and spinal cord neurons, for example, are clearly enlarged, other cell types were unchanged. This might be explained by a differential cell-autonomous effect from increased TORC1 signaling and expression of other components of TORC1. Moreover, despite some enlarged organs, the overall body size of the mutant larvae does not seem to be increased, again suggesting variable requirements for Tuberin in distinct cells and tissues during zebrafish development.

Zebrafish *tsc2* regulates cortical organization during development

Despite recent progress and the development of several rodent models of TSC, many important questions still remain about the role of *TSC1* and *TSC2* genes during development. In particular, the pathogenesis of tubers remains poorly understood. These brain malformations are almost universal manifestations in patients with TSC and probably underlie the severe neurological features of epilepsy and autism that are seen in these patients (Crino, 2004; Crino et al., 2006). In this study, we demonstrate that zebrafish that are homozygous for the *tsc2*^{vu242} allele have strikingly abnormal brain development with disorganization of the gray and white matter. These results are quite reminiscent of the cortical defects seen within human cortical tubers. It will be important in future studies to delineate the cellular basis of the forebrain abnormalities in *tsc2*$^{vu242/vu242}$ mutants and the relevance of these mechanisms to tubers seen in human TSC patients. In particular, it will be imperative to investigate whether ectopically positioned neurons within mutant forebrains arise via abnormal migration and/or abnormal differentiation. The transparent nature of zebrafish embryos coupled with the availability of multiple fluorescent-tagged proteins will greatly facilitate such analyses (Garcia-Lecea et al., 2008; Tsai et al., 2006).

Haploinsufficiency of *tsc2*

Whereas fish that are homozygous for the *tsc2*^{vu242} allele have overt multi-organ pathology, heterozygous fish are phenotypically normal. This broadly supports the prevailing model of TSC pathogenesis that an initial germline mutation in *TSC1* or *TSC2* is followed by a subsequent 'second-hit' in the remaining allele of either gene. This mechanism is consistent with an apparent requirement for homozygous inactivation of *Tsc1* or *Tsc2* in mouse models of TSC (Kobayashi et al., 1999; Onda et al., 1999). Mice heterozygous for *Tsc1* or *Tsc2* seem to undergo normal brain development without any abnormalities of neuronal layering or other structural lesions (Onda et al., 1999; Uhlmann et al., 2002a). However, an alternative mechanism to consider is haploinsufficiency, where the presence of only one functional copy of either *TSC1* or *TSC2* results in the pathological and clinical features of TSC. Broadly consistent with this notion, a moderate increase in mTORC1 signaling is seen in the hippocampus of *Tsc2* heterozygous mice, which have structurally normal brains. These animals were also shown to have deficits in hippocampus-dependent learning tasks, and these deficits were suppressed by rapamycin treatment (Ehninger et al., 2008). Whereas zebrafish heterozygous for the *tsc2*^{vu242} allele seem to undergo normal development and do not have enlarged cell size, they manifest moderately increased TORC1 signaling (Fig. 2; supplementary material Fig. S5). We reasoned that *tsc2*$^{vu242/+}$ heterozygous zebrafish might have decreased resistance to induced endoplasmic reticulum (ER) stress compared with wild-type zebrafish. Accordingly, we found that treatment with low doses of tunicamycin (to pharmacologically induce ER stress) significantly activated TORC1 signaling in *tsc2*$^{vu242/+}$ but not wild-type zebrafish (supplementary material Fig. S7). These results further support the concept that haploinsufficiency of *tsc2* when combined with physiological insults can lead to the elevation of TOR signaling past the threshold to trigger pathological changes. However, a dominant-negative activity of the truncated Tuberin cannot be excluded at this time.

Tuber pathogenesis in humans

It is unknown how directly relevant any results from *tsc2*^{vu242} mutant zebrafish are for patients with TSC. A subset of TSC patients clearly harbor *TSC2* mutations that inactivate or remove the GAP domain but retain the hamartin-binding domain (Sancak et al., 2005). Such alleles have not yet been examined for functional consequences in animal models. This reflects the technical difficulty in studying human genetic diseases in transgenic mouse models and underscores the need for additional model systems such as zebrafish.

tsc2$^{vu242/vu242}$ mutant cells exhibit a cell-autonomous increase of TOR1 activity when transplanted into wild-type zebrafish. However, we also observed that transplanted *tsc2*$^{vu242/vu242}$ mutant cells were able, in a non-cell-autonomous manner, to cause mislocalization of wild-type cells in the forebrain. This result is particularly interesting because it suggests that some cells that contribute to tuber formation in the brains of patients with TSC might retain a wild-type *TSC2* allele. The possible mechanism is unknown but might reasonably relate to factors secreted from mutant cells that alter the differentiation, migration or function of wild-type cells in the brain.

This new zebrafish model is well situated to begin to address many important questions in TSC and TOR biology and disease pathogenesis, and should complement studies that use rodent models. The conserved sequence and expression of zebrafish *tsc2* coupled with the multi-organ pathology seen in *tsc2*$^{vu242/vu242}$ homozygous zebrafish and their response to treatment with rapamycin further illustrate the utility of this model of TSC. Many questions remain about TSC pathogenesis and the role of the *TSC2* gene during brain development. The availability of this zebrafish model should facilitate new discoveries and catalyze the identification and testing of new therapies for neurological and non-neurological aspects of TSC.

METHODS

Fish strains

Zebrafish strains used in this study included AB*, *tsc2*^{vu242}, *Tg(β-actin:mGFP)* (Cooper et al., 2005) and *Tg(h2afv:GFP)* (Pauls et al., 2001). Embryos were obtained from natural matings and raised at 28.5°C in egg water (0.3 g of sea salts/l).

TILLING of *tsc2* gene and genotyping for the *tsc2*^{vu242} mutation

A nonsense mutation in the *tsc2* gene was isolated by screening 4608 F1 progeny of ENU-treated males using TILLING (supplementary material Fig. S1) (Till et al., 2003). A part of the tail was used for the genotyping of individual embryos after fixation in 4% paraformaldehyde. *tsc2*^{vu242} was maintained in the AB* genetic background. The mutation introduces a C3087 to A transversion, which abolishes an *Hpy*Ch4IV restriction-enzyme recognition site. For genotyping of *tsc2*^{vu242}, we amplified a 151-bp fragment by PCR using the forward primer 5′-CCAGCACC-ACCTGCAGTCTGG-3′ and reverse primer 5′-CTCTTGGGC-AGAGCAGAGAAGTTGG-3′ flanking the mutation site. Mutation was confirmed by absence of the *Hpy*Ch4IV restriction site.

RNA injection

Synthetic RNA was prepared, using mMessage mMachine kit (Ambion), from wild-type *tsc2*, mutant *tsc2*^{vu242} and a truncated form of *tsc2* generated by *Nru*I restriction-enzyme digestion. Capped mRNAs were diluted in 0.1 M KCl solution containing 0.5% Phenol Red. 200-400 pg aliquots of RNA were injected into one-cell-stage embryos using standard protocols.

Morpholino design and injection

3 ng of antisense morpholino oligonucleotide was injected into one-cell-stage embryos to verify antibody specificity of phospho-Tuberin (Ser939). MO-*tsc2* (5′-ACTCTTTACTGGGCTGTTT-ATTCAT-3′; GeneTools) was designed to specifically target the ATG start codon and inhibit translation of *tsc2*.

Whole-mount in situ hybridization

Embryos were fixed in 4% paraformaldehyde overnight and dehydrated in 100% methanol at –20°C. Whole-mount hybridization was performed using standard protocols (Jowett and Lettice, 1994). BCIP/NBT (Vector Laboratories) mixture was used as a chromogenic substrate. In situ images were acquired using a Zeiss Axioscope and Nikon COOLPIX 995 digital camera.

Immunofluorescence

Embryos were fixed in 4% paraformaldehyde from overnight to 2 days at 4°C. Fixed embryos were embedded in 1.2% agarose/5%

sucrose and saturated in 30% sucrose. Tissue blocks were frozen in 2-methylbutane chilled using liquid nitrogen. 10-µm sections were collected on microscope slides using a Leica cryostat. Sections were kept in –80°C before use. Sections were rehydrated in 1× PBS for 20 minutes at room temperature and blocked in 5% sheep serum/1× PBS for 1 hour. Sections were incubated with antibodies to phospho-S6 ribosomal protein (Cell Signaling #2215; Ser235/236; dilution 1:300), phospho-4E-BP1 (Cell Signaling #2855; Thr37/46; dilution 1:300) and phospho-Tuberin (Cell Signaling #3615; Ser939; dilution 1:300) overnight at 4°C, rinsed for 1 hour with PBS and then incubated overnight at 4°C with Cy3-labeled goat anti-rabbit secondary antibody (Jackson ImmunoResearch). Sections were then washed with 1× PBS for 1 hour and mounted in VECTASHIELD with DAPI (Vector Laboratories). Images were acquired using a Zeiss Axio Imager Z1 and Zeiss AxioCam MRm digital camera. Digital images were then processed using Adobe Photoshop CS2. All images received only minor modifications, with control and mutant sections always processed in parallel.

Cell size analysis and cell counting

To compare cell size, images of cross sections were obtained and the outline of each cell was drawn manually using ImageJ. The number of pixels where then measured in each cell. For neuronal cell counting, sections were stained with DAPI, images of cross-sections obtained from 12 different embryos and cells were manually counted in Adobe Photoshop. Statistical analyses were performed using Student's *t*-test.

Tunicamycin treatment

Tunicamycin (Sigma) was dissolved in dimethyl sulfoxide (DMSO) as 1 mg/ml concentration and diluted with egg water at a final concentration of 200 ng/ml and 400 ng/ml. Tunicamycin treatment started at 7 dpf and continued until 8.5 dpf.

Rapamycin treatment

A stock solution of rapamycin (30 mg/ml in 100% ethanol; LC Laboratories) was diluted with egg water. Rapamycin treatment was initiated between 3.5 dpf and continued until 7 dpf depending on the specific experiment. Rapamycin-containing water was replaced every 24 hours.

Embryo extract preparation and western blotting

A total of 20 embryos at 7 dpf were lysed by adding RIPA cell lysis buffer (18 µl per embryo of 10 mM Tris, pH 7.4, 150 mM NaCl, 1 mM EDTA, 0.1% SDS, 1% Triton X-100, 1% sodium deoxycholate) and pre-heated (100°C) in 4× Laemmli SDS sample reducing buffer (6 µl per embryo) (1×: 250 mM Tris-HCl, pH 6.8, 40% glycerol, 8% SDS, 20% β-mercaptoethanol, 0.004% Bromophenol Blue), then the tissue was macerated until suspended. For phospho-S6, lysates equaling 1.6 embryos were loaded per lane in a Tris-HCl 4-15% polyacrylamide gel. For phospho-4E-BP1, lysates equaling four embryos were loaded per lane in a Tris-HCl 18% polyacrylamide gel. The gels were run using the Bio-Rad Criterion system according to the manufacturer's instructions. The gels were transferred onto polyvinylidene fluoride (PVDF) membranes. Subsequent blocking, antibody incubation and film exposure were performed according to the manufacturer's recommendations. The antibodies used included anti-phospho-S6 ribosomal protein (Ser235/236; #4856, 2F9, Cell Signaling Technology; 1:1000), anti-4E-BP1 (#9644, 53H11, Cell Signaling Technology; 1:1000) and anti-β-actin as a loading control (#A5441, Sigma-Aldrich; 1:2000).

TRANSLATIONAL IMPACT

Clinical issue

Tuberous sclerosis complex (TSC) is a multi-organ disease caused by mutations in either of the *TSC1* or *TSC2* genes, the products of which act as repressors of a fundamentally important kinase, mTORC1. Patients with TSC develop hamartomas (benign tumor-like overgrowths of normal mature cells) in the brain, kidney, skin, lung and heart. Brain hamartomas (known as 'tubers') are thought to cause the neurological manifestations of the disease, which include epilepsy, autism, mental retardation and psychiatric problems. Disease prognosis depends on the severity of the symptoms, which range from mild skin abnormalities to severe mental retardation, seizures and kidney failure. There is no cure, although mTORC1 inhibitors are currently being tested in clinical trials as a 'rational' therapeutic. Although mouse and rat models of TSC exist, many fundamental questions regarding the mechanisms of disease initiation and progression remain, particularly with respect to the development of brain tubers.

Results

The authors develop a model system of TSC by introducing a premature stop codon in the zebrafish *tsc2* gene (which encodes the protein tuberin). This $tsc2^{vu242}$ allele prevents translation of the GTPase-activating protein (GAP) domain of tuberin, which is known to be required for TORC1 inhibition. Zebrafish homozygous for the $tsc2^{vu242}$ mutation die at larval stages and have increased TORC1 signaling, abnormally large cells in the brain and liver, and forebrain disorganization. Heterozygous $tsc2^{vu242}$ zebrafish have slight increases in TORC1 signaling but no abnormalities in cell size or tissue organization. Treatment of homozygous $tsc2^{vu242}$ zebrafish with rapamycin, a potent and specific inhibitor of the TORC1 complex, reverses signaling abnormalities and restores cell size to normal. In transplantation experiments, *tsc2*-deficient cells have increased TORC1 signaling in a cell-autonomous manner, as expected. However, non-cell-autonomous effects are also observed, because mutant cells can recruit wild-type cells to ectopic regions of the host forebrain.

Implications and future directions

Although the precise roles of *TSC1* and *TSC2* genes during normal development, as well as during hamartoma formation in patients with TSC, remain elusive, it is clear that control of mTORC1 signaling is highly important for many aspects of the disease. This zebrafish model of TSC will enhance understanding of normal tuberin function, and of the cell-autonomous and non-cell-autonomous mechanisms required for the development of hamartomas in patients with TSC. Future approaches using this model system will include investigation of key genetic interactions and screening for compounds that can modulate TOR-dependent and -independent signaling pathways.

doi:10.1242/dmm.006932

Chimeric analysis

We used $tsc2^{vu242}$*;Tg(β-actin:mGFP)* and tsc^{vu242}*;Tg(h2afv:GFP)* lines for chimeric analysis by transplantation. 30-50 blastomeres from donors obtained by crossing $tsc2^{vu242}$*;Tg(β-actin:mGFP)* or $tsc2^{vu242}$*;Tg(h2afv:GFP)* fish were transplanted at 4 hpf into same-stage wild-type hosts. Host embryos were raised at 28.5°C. 1-year-old adult chimeric fish were euthanized by 20% 3-aminobenzoic acid ethyl ester (MESAB; Sigma); brains were then fixed in 4% PFA for analysis. Donor embryos expressing GFP-positive cells were fixed at 1 dpf and genotyped for $tsc2^{vu242}$ mutation. Host embryos and adult brains were mounted in 1.2% agarose/5% sucrose as

described above. After determination of donor genotypes, 10-μm transverse sections of fixed chimeric embryos were collected using a Leica CM1900 cryostat microtome. Sections were stained with the anti-phospho-S6 antibody and mounted in VECTASHIELD with DAPI as described above and imaged using Zeiss Axio Imager Z1 or Zeiss AxioCam MRm digital cameras.

ACKNOWLEDGEMENTS

We thank L.S.-K. group members for discussions and for critically reading the manuscript. We thank our fish facility staff for excellent care. This work in the L.S.-K. lab was supported by the Zebrafish Initiative – Vanderbilt University Academic Capital Venture Fund and Martha Rivers Ingram Endowed Chair. K.C.E. was supported by the NINDS, NIH and the Tuberous Sclerosis Alliance.

COMPETING INTERESTS

The authors declare no financial or competing interests.

AUTHOR CONTRIBUTIONS

S.-H.K. developed the concept, performed experiments and prepared the manuscript, C.K.S. performed experiments, L.S.-K. developed the approach and edited the manuscript, and K.C.E. developed the approach and edited the manuscript.

SUPPLEMENTARY MATERIAL

Supplementary material for this article is available at
http://dmm.biologists.org/lookup/suppl/doi:10.1242/dmm.005587/-/DC1

Note added in proof

While this manuscript was under revision, a report of 'second-hit' mutations in single cells obtained from human tubers was published (Crino et al., 2010). On the basis of their results, these authors also suggest that cell-autonomous and non-cell-autonomous mechanisms are operative during the pathogenesis of tubers. A further recent study using deep sequencing of the *TSC1* and *TSC2* genes also found second hits in human tubers but concluded that these were a rare occurrence (Qin et al., 2010).

REFERENCES

Au, K. S., Williams, A. T., Roach, E. S., Batchelor, L., Sparagana, S. P., Delgado, M. R., Wheless, J. W., Baumgartner, J. E., Roa, B. B., Wilson, C. M. et al. (2007). Genotype/phenotype correlation in 325 individuals referred for a diagnosis of tuberous sclerosis complex in the United States. *Genet. Med.* **9**, 88-100.

Baraban, S. C., Dinday, M. T., Castro, P. A., Chege, S., Guyenet, S. and Taylor, M. R. (2007). A large-scale mutagenesis screen to identify seizure-resistant zebrafish. *Epilepsia* **48**, 1151-1157.

Bissler, J. J., McCormack, F. X., Young, L. R., Elwing, J. M., Chuck, G., Leonard, J. M., Schmithorst, V. J., Laor, T., Brody, A. S., Bean, J. et al. (2008). Sirolimus for angiomyolipoma in tuberous sclerosis complex or lymphangioleiomyomatosis. *N. Engl. J. Med.* **358**, 140-151.

Bourneville, D. M. (1880). Tuberous sclerosis with cortical abnormalities: mental retardation and hemiplegic epilepsy. *Arch. Neurol.* **1**, 81-91.

Cooper, M. S., Szeto, D. P., Sommers-Herivel, G., Topczewski, J., Solnica-Krezel, L., Kang, H. C., Johnson, I. and Kimelman, D. (2005). Visualizing morphogenesis in transgenic zebrafish embryos using BODIPY TR methyl ester dye as a vital counterstain for GFP. *Dev. Dyn.* **232**, 359-368.

Crino, P. B. (2004). Molecular pathogenesis of tuber formation in tuberous sclerosis complex. *J. Child Neurol.* **19**, 716-725.

Crino, P. B., Nathanson, K. L. and Henske, E. P. (2006). The tuberous sclerosis complex. *N. Engl. J. Med.* **355**, 1345-1356.

Crino, P., Aronica, E., Baltuch, G. and Nathanson, K. (2010). Biallelic TSC gene inactivation in tuberous sclerosis complex. *Neurology* **74**, 1716-1723.

Davies, D. M., Johnson, S. R., Tattersfield, A. E., Kingswood, J. C., Cox, J. A., McCartney, D. L., Doyle, T., Elmslie, F., Saggar, A., de Vries, P. J. et al. (2008). Sirolimus therapy in tuberous sclerosis or sporadic lymphangioleiomyomatosis. *N. Engl. J. Med.* **358**, 200-203.

DiBella, L. M., Park, A. and Sun, Z. (2009). Zebrafish Tsc1 reveals functional interactions between the cilium and the TOR pathway. *Hum. Mol. Genet.* **18**, 595-606.

Ehninger, D., Han, S., Shilyansky, C., Zhou, Y., Li, W., Kwiatkowski, D. J., Ramesh, V. and Silva, A. J. (2008). Reversal of learning deficits in a Tsc2+/- mouse model of tuberous sclerosis. *Nat. Med.* **14**, 843-848.

Ess, K. C. (2006). The neurobiology of tuberous sclerosis complex. *Semin. Pediatr. Neurol.* **13**, 37-42.

Franz, D. N., Leonard, J., Tudor, C., Chuck, G., Care, M., Sethuraman, G., Dinopoulos, A., Thomas, G. and Crone, K. R. (2006). Rapamycin causes regression of astrocytomas in tuberous sclerosis complex. *Ann. Neurol.* **59**, 490-498.

Garcia-Lecea, M., Kondrychyn, I., Fong, S. H., Ye, Z. R. and Korzh, V. (2008). In vivo analysis of choroid plexus morphogenesis in zebrafish. *PLoS ONE* **3**, e3090.

Govindarajan, B., Brat, D. J., Csete, M., Martin, W. D., Murad, E., Litani, K., Cohen, C., Cerimele, F., Nunnelley, M., Lefkove, B. et al. (2005). Transgenic expression of dominant negative tuberin through a strong constitutive promoter results in a tissue-specific tuberous sclerosis phenotype in the skin and brain. *J. Biol. Chem.* **280**, 5870-5874.

Henske, E. P., Scheithauer, B. W., Short, M. P., Wollmann, R., Nahmias, J., Hornigold, N., van Slegtenhorst, M., Welsh, C. T. and Kwiatkowski, D. J. (1996). Allelic loss is frequent in tuberous sclerosis kidney lesions but rare in brain lesions. *Am. J. Hum. Genet.* **59**, 400-406.

Huang, J. and Manning, B. D. (2008). The TSC1-TSC2 complex: a molecular switchboard controlling cell growth. *Biochem. J.* **412**, 179-190.

Huang, J. and Manning, B. D. (2009). A complex interplay between Akt, TSC2 and the two mTOR complexes. *Biochem. Soc. Trans.* **37**, 217-222.

Inoki, K., Li, Y., Zhu, T., Wu, J. and Guan, K. L. (2002). TSC2 is phosphorylated and inhibited by Akt and suppresses mTOR signalling. *Nat. Cell Biol.* **4**, 648-657.

Inoki, K., Li, Y., Xu, T. and Guan, K. L. (2003). Rheb GTPase is a direct target of TSC2 GAP activity and regulates mTOR signaling. *Genes Dev.* **17**, 1829-1834.

Jowett, T. and Lettice, L. (1994). Whole-mount in situ hybridizations on zebrafish embryos using a mixture of digoxigenin- and fluorescein-labelled probes. *Trends Genet.* **10**, 73-74.

Kobayashi, T., Hirayama, Y., Kobayashi, E., Kubo, Y. and Hino, O. (1995). A germline insertion in the tuberous sclerosis (Tsc2) gene gives rise to the Eker rat model of dominantly inherited cancer. *Nat. Genet.* **9**, 70-74.

Kobayashi, T., Minowa, O., Kuno, J., Mitani, H., Hino, O. and Noda, T. (1999). Renal carcinogenesis, hepatic hemangiomatosis, and embryonic lethality caused by a germ-line Tsc2 mutation in mice. *Cancer Res.* **59**, 1206-1211.

Kobayashi, T., Minowa, O., Sugitani, Y., Takai, S., Mitani, H., Kobayashi, E., Noda, T. and Hino, O. (2001). A germ-line Tsc1 mutation causes tumor development and embryonic lethality that are similar, but not identical to, those caused by Tsc2 mutation in mice. *Proc. Natl. Acad. Sci. USA* **98**, 8762-8767.

Ma, L., Chen, Z., Erdjument-Bromage, H., Tempst, P. and Pandolfi, P. P. (2005). Phosphorylation and functional inactivation of TSC2 by Erk implications for tuberous sclerosis and cancer pathogenesis. *Cell* **121**, 179-193.

Makky, K., Tekiela, J. and Mayer, A. N. (2007). Target of rapamycin (TOR) signaling controls epithelial morphogenesis in the vertebrate intestine. *Dev. Biol.* **303**, 501-513.

Meikle, L., McMullen, J. R., Sherwood, M. C., Lader, A. S., Walker, V., Chan, J. A. and Kwiatkowski, D. J. (2005). A mouse model of cardiac rhabdomyoma generated by loss of Tsc1 in ventricular myocytes. *Hum. Mol. Genet.* **14**, 429-435.

Meikle, L., Pollizzi, K., Egnor, A., Kramvis, I., Lane, H., Sahin, M. and Kwiatkowski, D. J. (2008). Response of a neuronal model of tuberous sclerosis to mammalian target of rapamycin (mTOR) inhibitors: effects on mTORC1 and Akt signaling lead to improved survival and function. *J. Neurosci.* **28**, 5422-5432.

Mizuguchi, M. T. S. (2001). Neuropathology of tuberous sclerosis. *Brain Dev.* **23**, 508-515.

Mueller, T. and Wullimann, M. F. (2009). An evolutionary interpretation of teleostean forebrain anatomy. *Brain Behav. Evol.* **74**, 30-42.

Mullins, M. C., Hammerschmidt, M., Haffter, P. and Nusslein-Volhard, C. (1994). Large-scale mutagenesis in the zebrafish: in search of genes controlling development in a vertebrate. *Curr. Biol.* **4**, 189-202.

Nobukini, T. and Thomas, G. (2004). The mTOR/S6K signalling pathway: the role of the TSC1/2 tumour suppressor complex and the proto-oncogene Rheb. *Novartis Found. Symp.* **262**, 148-154; discussion 154-159, 265-268.

Onda, H., Lueck, A., Marks, P. W., Warren, H. B. and Kwiatkowski, D. J. (1999). Tsc2(+/-) mice develop tumors in multiple sites that express gelsolin and are influenced by genetic background. *J. Clin. Invest.* **104**, 687-695.

Park, S. H., Pepkowitz, S. H., Kerfoot, C., De Rosa, M. J., Poukens, V., Wienecke, R., DeClue, J. E. and Vinters, H. V. (1997). Tuberous sclerosis in a 20-week gestation fetus: immunohistochemical study. *Acta Neuropathol.* **94**, 180-186.

Pauls, S., Geldmacher-Voss, B. and Campos-Ortega, J. A. (2001). A zebrafish histone variant H2A.F/Z and a transgenic H2A.F/Z:GFP fusion protein for in vivo studies of embryonic development. *Dev. Genes Evol.* **211**, 603-610.

Qin, W., Chan, J. A., Vinters, H. V., Mathern, G. W., Franz, D. N., Taillon, B. E., Bouffard, P. and Kwiatkowski, D. J. (2010). Analysis of TSC cortical tubers by deep sequencing of TSC1, TSC2 and KRAS demonstrates that small second-hit mutations in these genes are rare events. *Brain Pathol.* Epub ahead of print.

Sancak, O., Nellist, M., Goedbloed, M., Elfferich, P., Wouters, C., Maat-Kievit, A., Zonnenberg, B., Verhoef, S., Halley, D. and van den Ouweland, A. (2005). Mutational analysis of the TSC1 and TSC2 genes in a diagnostic setting: genotype-

phenotype correlations and comparison of diagnostic DNA techniques in Tuberous Sclerosis Complex. *Eur. J. Hum. Genet.* **13**, 731-741.

Shepherd, C. W., Houser, O. W. and Gomez, M. R. (1995). MR findings in tuberous sclerosis complex and correlation with seizure development and mental impairment. *Am. J. Neuroradiol.* **16**, 149-155.

Silva, A. L. and Romao, L. (2009). The mammalian nonsense-mediated mRNA decay pathway: to decay or not to decay! Which players make the decision? *FEBS Lett.* **583**, 499-505.

Solnica-Krezel, L., Schier, A. F. and Driever, W. (1994). Efficient recovery of ENU-induced mutations from the zebrafish germline. *Genetics* **136**, 1401-1420.

Tadros, W. and Lipshitz, H. D. (2009). The maternal-to-zygotic transition: a play in two acts. *Development* **136**, 3033-3042.

Talos, D. M., Kwiatkowski, D. J., Cordero, K., Black, P. M. and Jensen, F. E. (2008). Cell-specific alterations of glutamate receptor expression in tuberous sclerosis complex cortical tubers. *Ann. Neurol.* **63**, 454-465.

Till, B. J., Reynolds, S. H., Greene, E. A., Codomo, C. A., Enns, L. C., Johnson, J. E., Burtner, C., Odden, A. R., Young, K., Taylor, N. E. et al. (2003). Large-scale discovery of induced point mutations with high-throughput TILLING. *Genome Res.* **13**, 524-530.

Tsai, T. H., Lin, C. Y., Tsai, H. J., Chen, S. Y., Tai, S. P., Lin, K. H. and Sun, C. K. (2006). Biomolecular imaging based on far-red fluorescent protein with a high two-photon excitation action cross section. *Opt. Lett.* **31**, 930-932.

Tschuluun, N., Wenzel, H. J. and Schwartzkroin, P. A. (2007). Irradiation exacerbates cortical cytopathology in the Eker rat model of tuberous sclerosis complex, but does not induce hyperexcitability. *Epilepsy Res.* **73**, 53-64.

Uhlmann, E. J., Apicelli, A. J., Baldwin, R. L., Burke, S. P., Bajenaru, M. L., Onda, H., Kwiatkowski, D. and Gutmann, D. H. (2002a). Heterozygosity for the tuberous sclerosis complex (TSC) gene products results in increased astrocyte numbers and decreased p27-Kip1 expression in TSC2+/- cells. *Oncogene* **21**, 4050-4059.

Uhlmann, E. J., Wong, M., Baldwin, R. L., Bajenaru, M. L., Onda, H., Kwiatkowski, D. J., Yamada, K. and Gutmann, D. H. (2002b). Astrocyte-specific TSC1 conditional knockout mice exhibit abnormal neuronal organization and seizures. *Ann. Neurol.* **52**, 285-296.

van Slegtenhorst, M., Carr, E., Stoyanova, R., Kruger, W. D. and Henske, E. P. (2004). Tsc1+ and tsc2+ regulate arginine uptake and metabolism in Schizosaccharomyces pombe. *J. Biol. Chem.* **279**, 12706-12713.

Way, S. W., McKenna, J., 3rd, Mietzsch, U., Reith, R. M., Wu, H. C. and Gambello, M. J. (2009). Loss of Tsc2 in radial glia models the brain pathology of tuberous sclerosis complex in the mouse. *Hum. Mol. Genet.* **18**, 1252-1265.

Wong, M. (2008). Mechanisms of epileptogenesis in tuberous sclerosis complex and related malformations of cortical development with abnormal glioneuronal proliferation. *Epilepsia* **49**, 8-21.

Wong, M., Ess, K. C., Uhlmann, E. J., Jansen, L. A., Li, W., Crino, P. B., Mennerick, S., Yamada, K. A. and Gutmann, D. H. (2003). Impaired glial glutamate transport in a mouse tuberous sclerosis epilepsy model. *Ann. Neurol.* **54**, 251-256.

Woo, K. and Fraser, S. E. (1995). Order and coherence in the fate map of the zebrafish nervous system. *Development* **121**, 2595-2609.

Zeng, L. H., Xu, L., Gutmann, D. H. and Wong, M. (2008). Rapamycin prevents epilepsy in a mouse model of tuberous sclerosis complex. *Ann. Neurol.* **63**, 444-453.

Zhang, Y., Gao, X., Saucedo, L. J., Ru, B., Edgar, B. A. and Pan, D. (2003). Rheb is a direct target of the tuberous sclerosis tumour suppressor proteins. *Nat. Cell Biol.* **5**, 578-581.

Zhou, J., Blundell, J., Ogawa, S., Kwon, C. H., Zhang, W., Sinton, C., Powell, C. M. and Parada, L. F. (2009). Pharmacological inhibition of mTORC1 suppresses anatomical, cellular, and behavioral abnormalities in neural-specific Pten knock-out mice. *J. Neurosci.* **29**, 1773-1783.

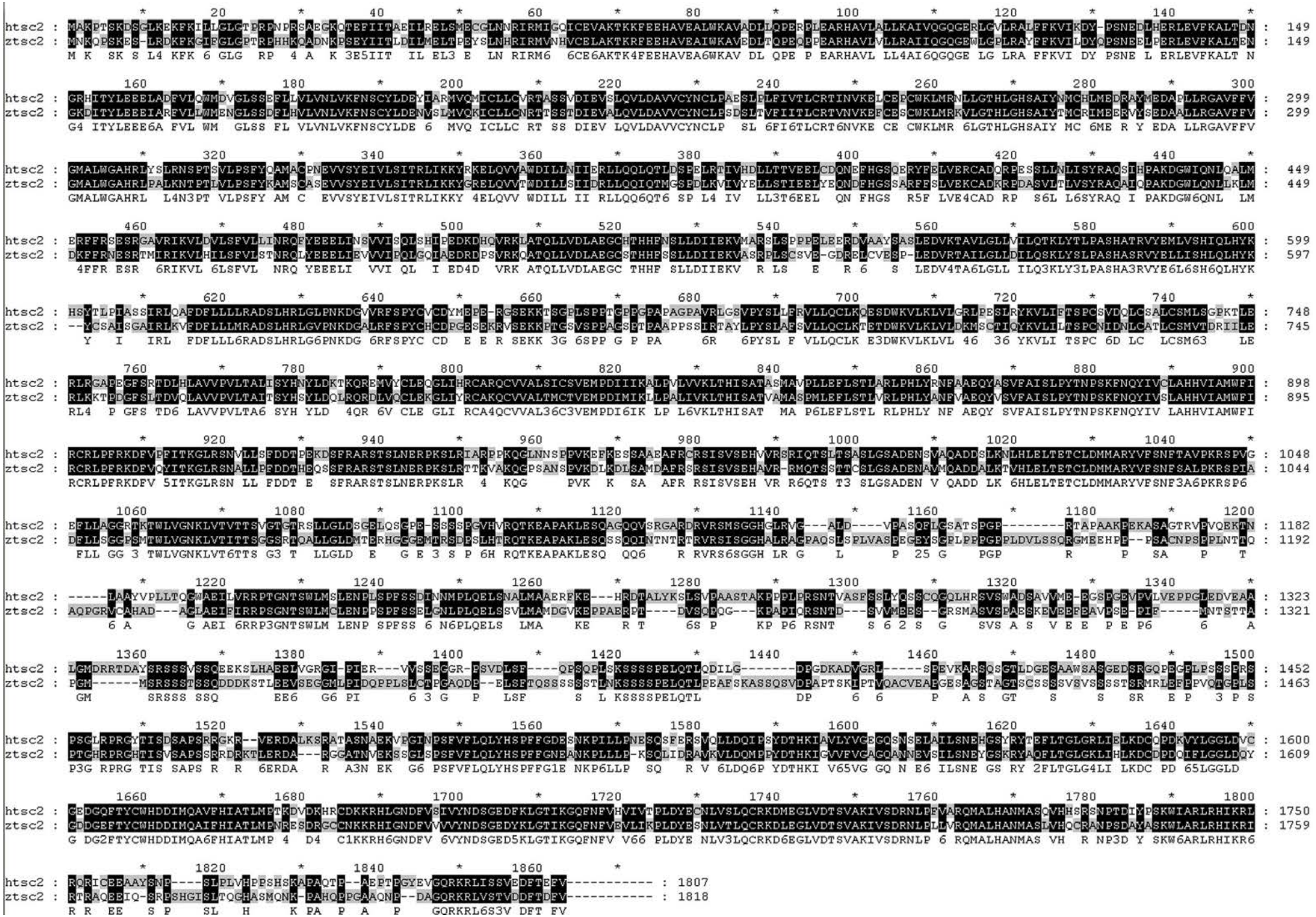

TILLING strategy for mutants screening in Zebrafish

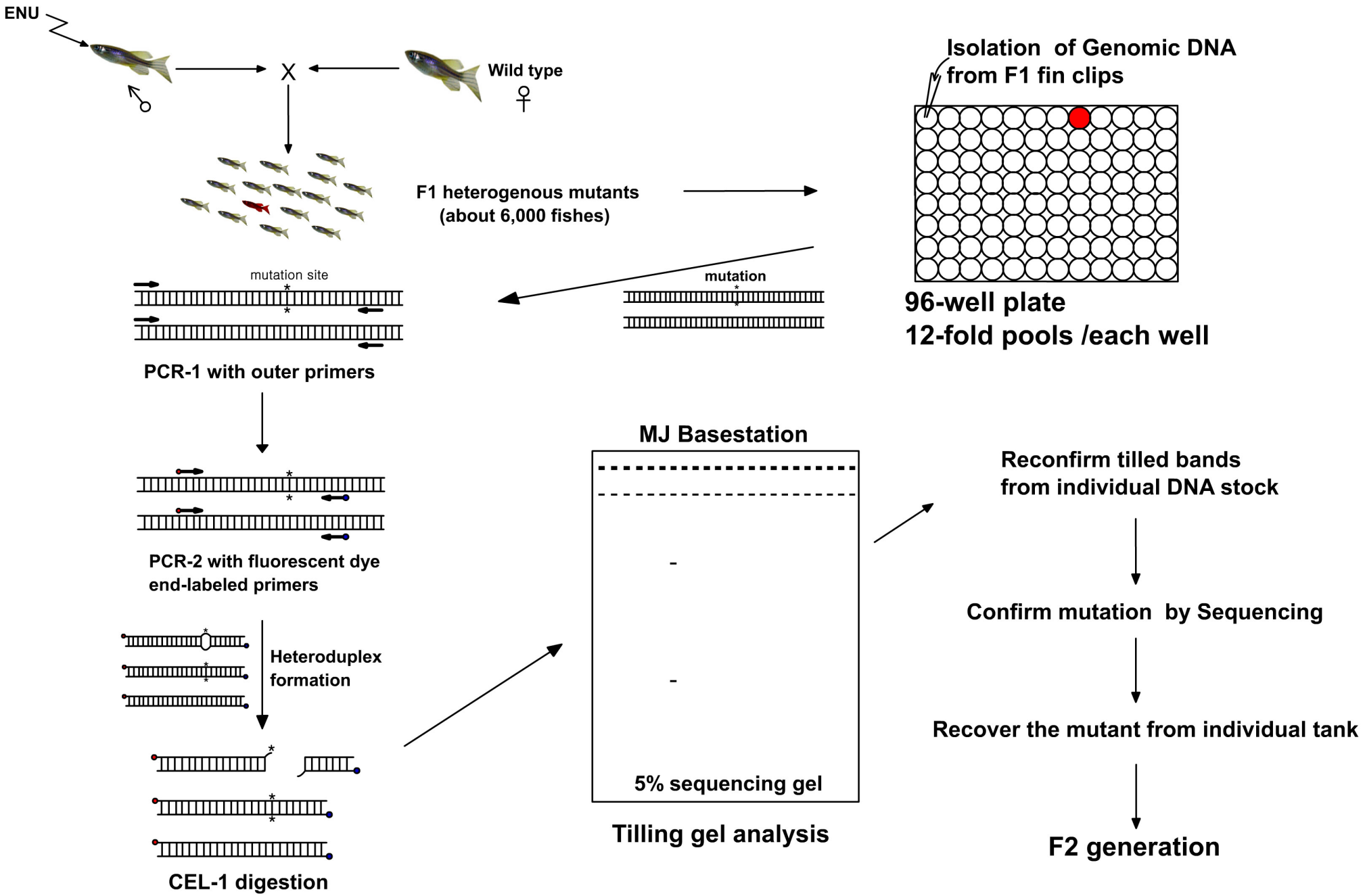

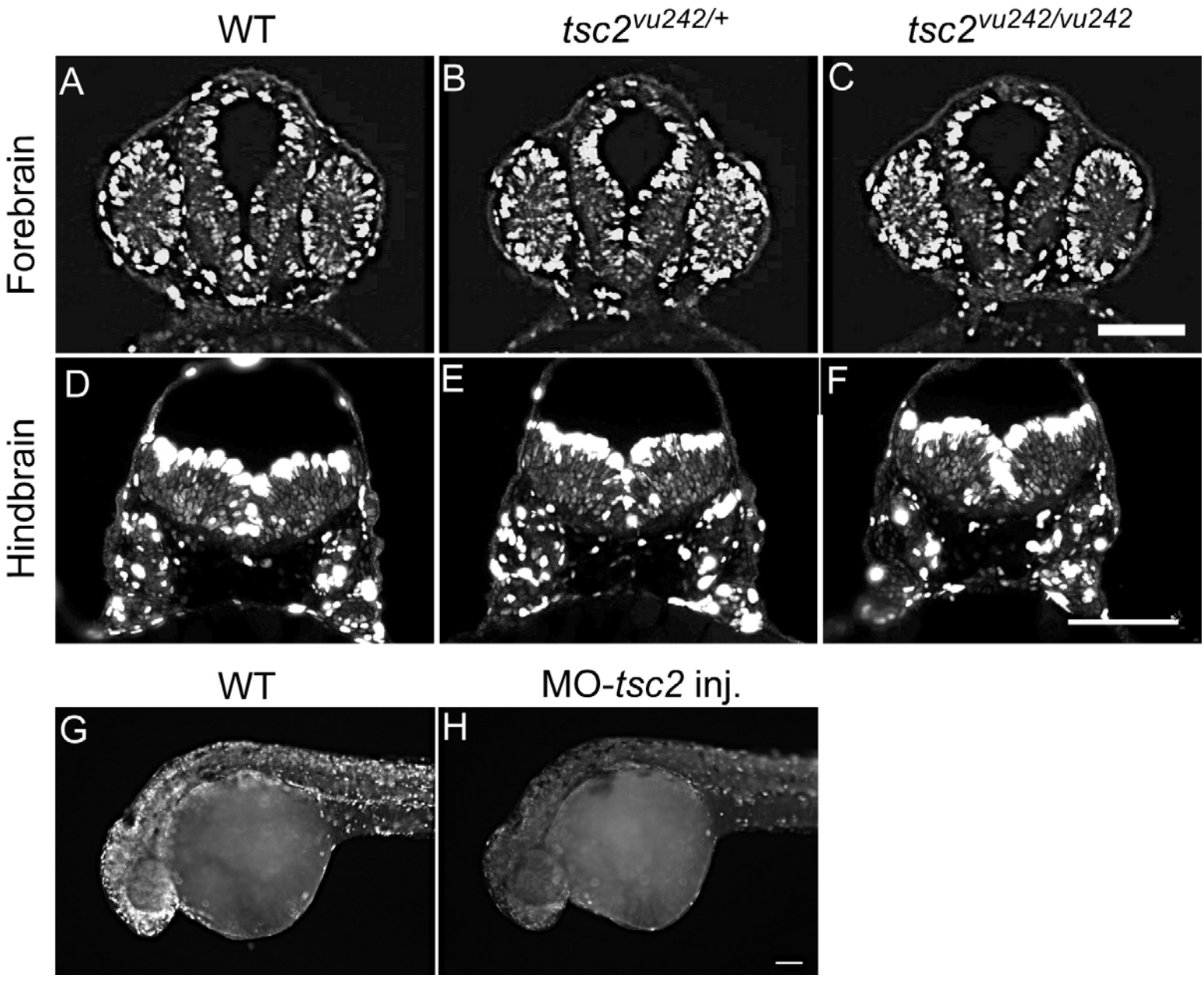
WT
tsc2vu242/+
tsc2vu242/vu242
Forebrain
Hindbrain
A
B
C
D
E
F
WT
MO-tsc2 inj.
G
H

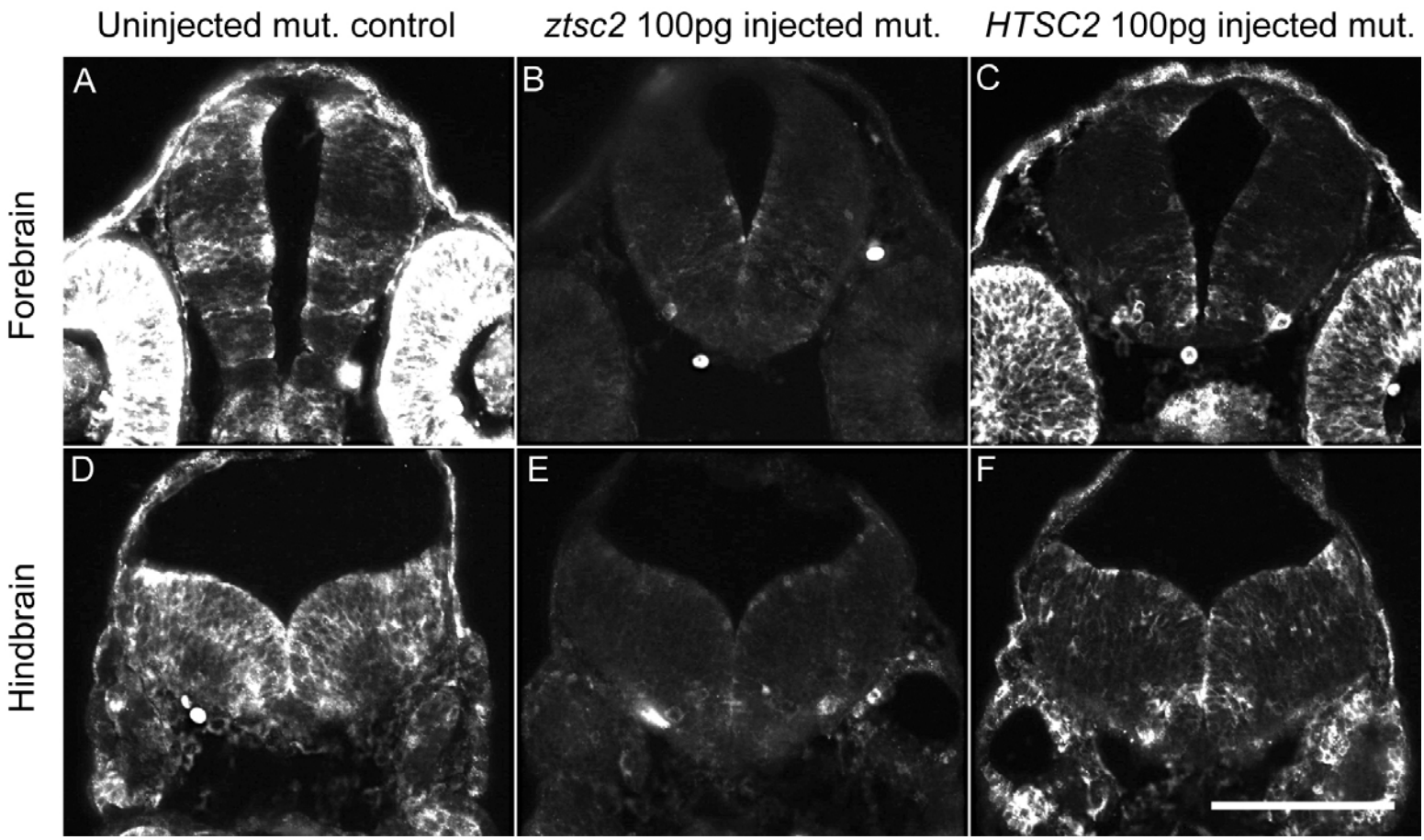
Uninjected mut. control
ztsc2 100pg injected mut.
HTSC2 100pg injected mut.
Forebrain
Hindbrain
A
B
C
D
E
F

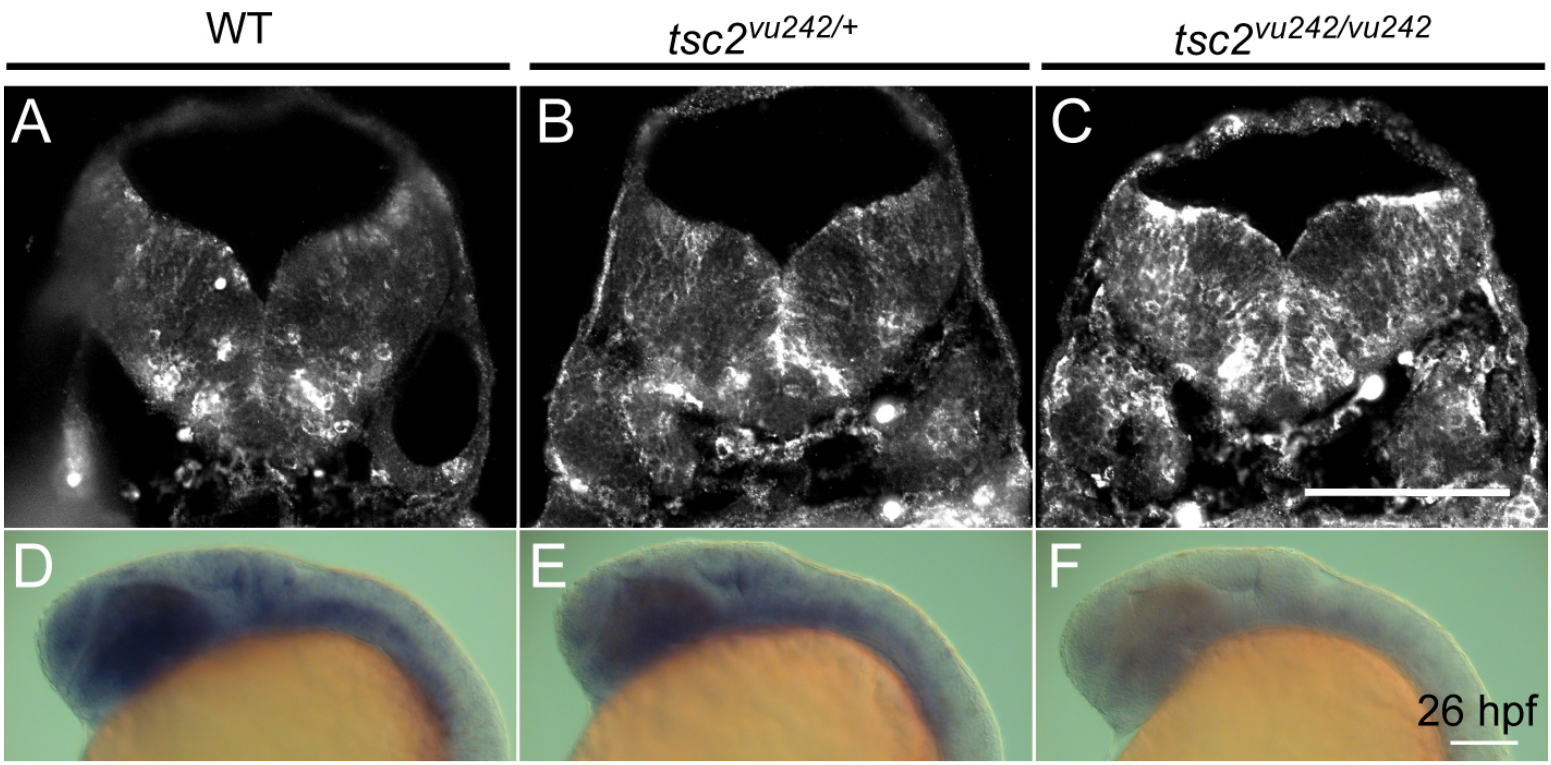
WT
tsc2vu242/+
tsc2vu242/vu242
A
B
C
D
E
F
26 hpf

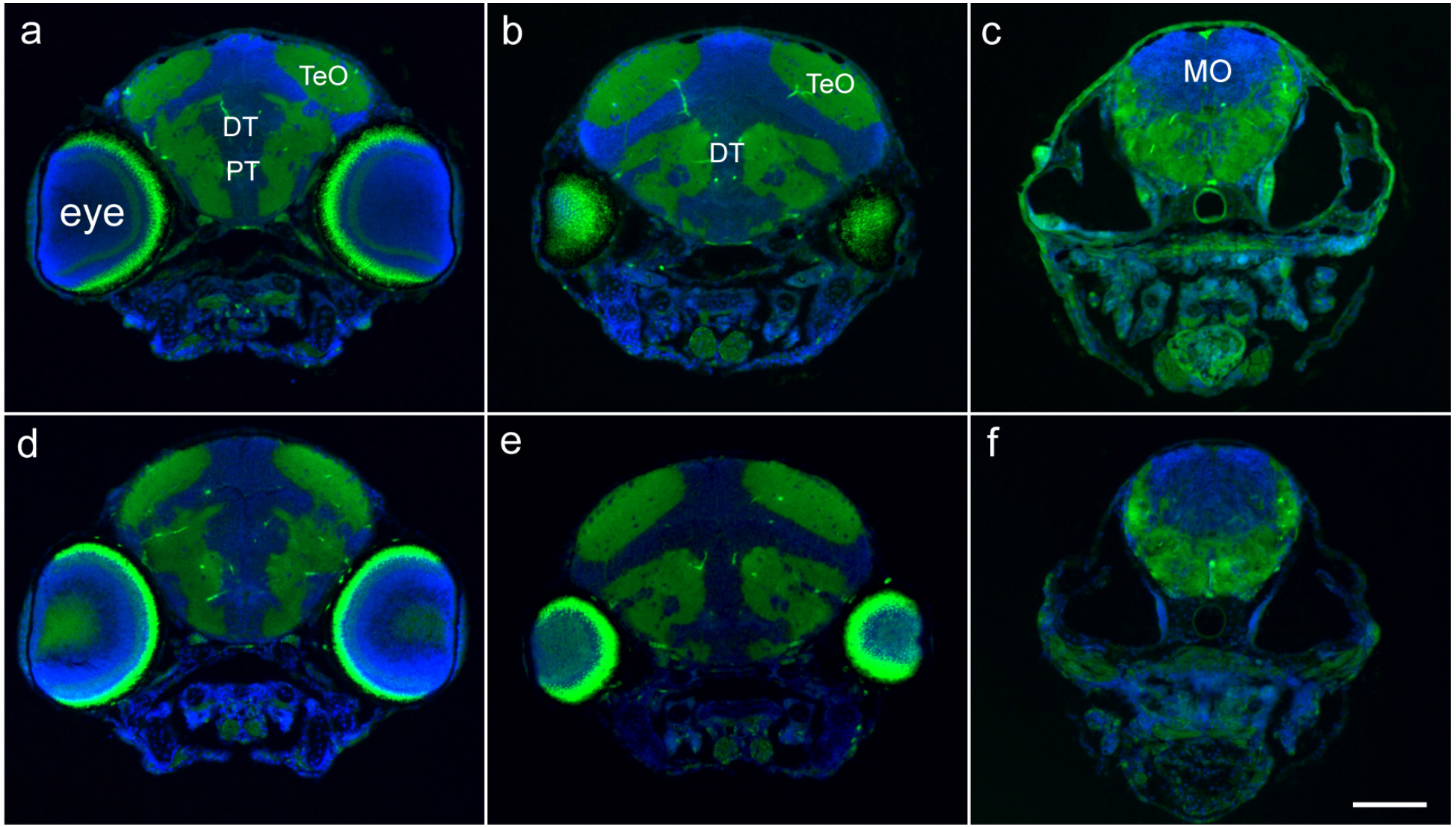
a
TeO
DT
PT
eye
b
TeO
DT
c
MO
WT
d
e
f
tsc2 vu242/vu242

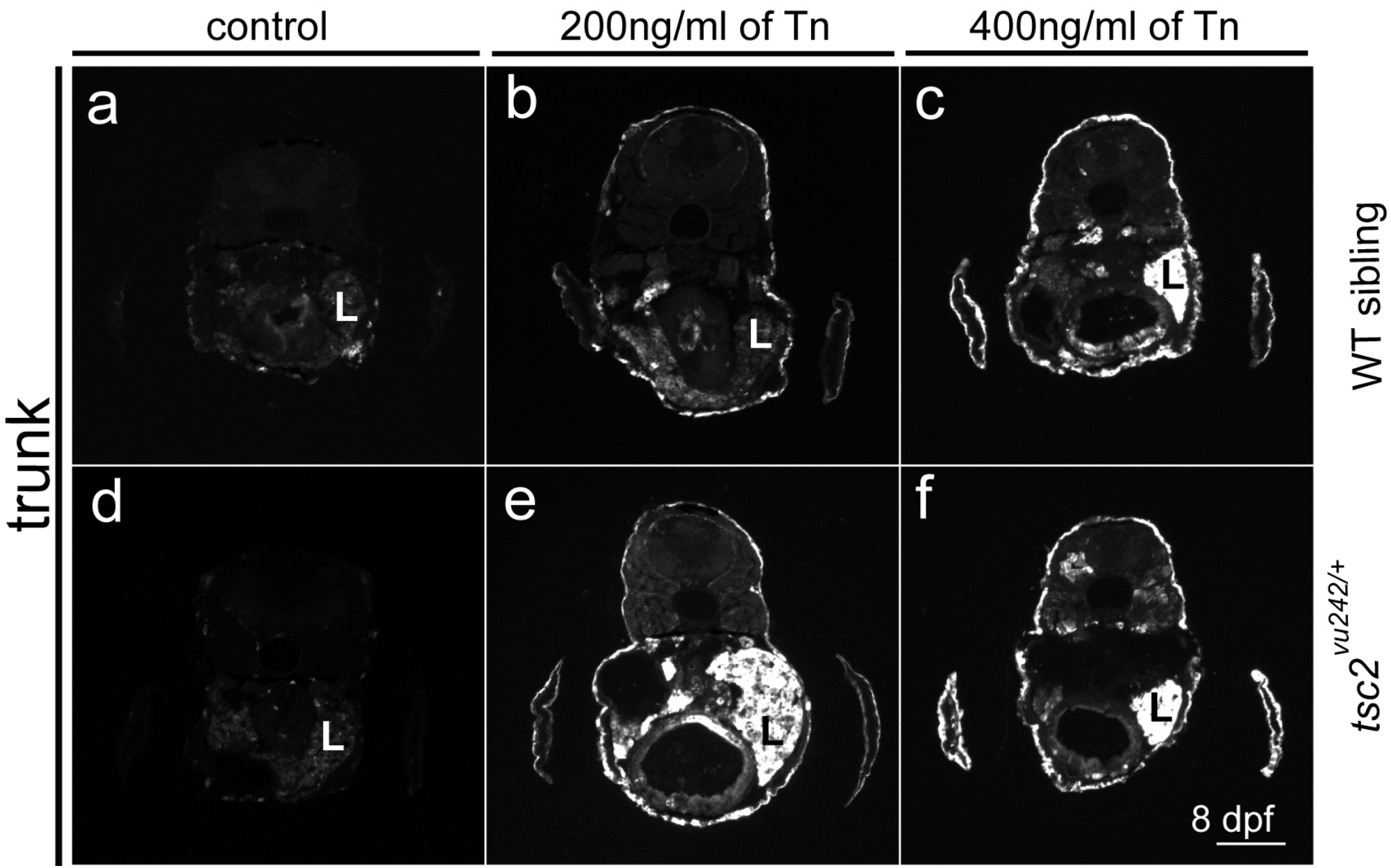
control
200ng/ml of Tn
400ng/ml of Tn
trunk
a
b
c
d
e
f
L
WT sibling
tsc2vu242/+
8 dpf